



PUBLISHED FOR SISSA BY SPRINGER

RECEIVED: April 29, 2010

REVISED: September 2, 2010

ACCEPTED: September 20, 2010

PUBLISHED: October 19, 2010

Predictions for Higgs production at the Tevatron and the associated uncertainties

Julien Baglio^a and Abdelhak Djouadi^{b,1}

^aLaboratoire de Physique Théorique, Université Paris-Sud XI et CNRS,
F-91405 Orsay Cedex, France

^bTheory Unit, CERN,
1211 Genève 23, Switzerland

E-mail: Julien.Baglio@th.u-psud.fr, Abdelhak.Djouadi@cern.ch

ABSTRACT: We update the theoretical predictions for the production cross sections of the Standard Model Higgs boson at the Fermilab Tevatron collider, focusing on the two main search channels, the gluon-gluon fusion mechanism $gg \rightarrow H$ and the Higgs-strahlung processes $q\bar{q} \rightarrow VH$ with $V = W/Z$, including all relevant higher order QCD and electroweak corrections in perturbation theory. We then estimate the various uncertainties affecting these predictions: the scale uncertainties which are viewed as a measure of the unknown higher order effects, the uncertainties from the parton distribution functions and the related errors on the strong coupling constant, as well as the uncertainties due to the use of an effective theory approach in the determination of the radiative corrections in the $gg \rightarrow H$ process at next-to-next-to-leading order. We find that while the cross sections are well under control in the Higgs-strahlung processes, the theoretical uncertainties are rather large in the case of the gluon-gluon fusion channel, possibly shifting the central values of the next-to-next-to-leading order cross sections by more than $\approx 40\%$. These uncertainties are thus significantly larger than the $\approx 10\%$ error assumed by the CDF and D0 experiments in their recent analysis that has excluded the Higgs mass range $M_H = 162\text{--}166$ GeV at the 95% confidence level. These exclusion limits should be, therefore, reconsidered in the light of these large theoretical uncertainties.

KEYWORDS: Higgs Physics, Hadronic Colliders, QCD, Standard Model

ARXIV EPRINT: [1003.4266](https://arxiv.org/abs/1003.4266)

¹Permanent address: Laboratoire de Physique Théorique, Unité mixte CNRS et Université Paris-Sud XI, F-91405 Orsay Cedex, France.

Contents

1	Introduction	1
2	The production cross sections	5
3	Theoretical uncertainties in gluon-gluon fusion	9
3.1	The scale uncertainty and higher order effects	9
3.2	Uncertainties due to the effective approach	16
3.3	Uncertainties from the PDFs and α_s	19
4	Theoretical uncertainties in Higgs-strahlung	26
5	The total uncertainties at the Tevatron	29
6	Conclusion	35
7	Addendum	37
7.1	The normalization of the $gg \rightarrow H$ cross section	37
7.2	The scale uncertainty	38
7.3	PDF and α_s uncertainties	40
7.4	Combination of the various uncertainties	42
7.5	Summary	43

1 Introduction

We are approaching the exciting and long awaited times of discovering the “Holy Grail” of nowadays particle physics: the Higgs boson [1–4], for a review see [5], the remnant of the mechanism breaking the electroweak gauge symmetry and at the origin of the particle masses. Indeed, the Large Hadron Collider (LHC) has started to have its first collisions [6], although at energies and with instantaneous luminosities yet far from those which would be required for discovery. Most importantly in this context, the CDF and D0 experiments at the Fermilab Tevatron collider have collected enough data to be sensitive to the Higgs particle of the Standard Model. Very recently, the two collaborations performed a combined analysis on the search for this particle and excluded at the 95% confidence level the possibility of a Higgs boson in the mass range between 162 and 166 GeV [7]; this exclusion range is expected to increase to $159 \text{ GeV} \leq M_H \leq 168 \text{ GeV}$ [8]. We are thus entering a new era in the quest of the Higgs particle as this is the first time that the mass range excluded by the LEP collaborations in the late 1990s, $M_H \geq 114.4 \text{ GeV}$ [9], is extended.

However, in contrast to the Higgs LEP limit which is rather robust, as the production cross section is mainly sensitive to small electroweak effects that are well under control,

the Tevatron exclusion limit critically depends on the theoretical prediction for the Higgs production cross sections which, at hadron colliders, are known to be plagued with various uncertainties. Among these are the contributions of yet uncalculated higher order corrections which can be important as the strong coupling constant α_s is rather large, the errors due to the folding of the partonic cross sections with the parton distribution functions (PDFs) to obtain the production rates at the hadronic level, and the errors on some important input parameters such as α_s . It is then mandatory to estimate these uncertainties in order to have a reliable theoretical prediction for the production rates, that would allow for a consistent confrontation between theoretical results and experimental measurements or exclusion bounds.¹ The present paper critically addresses this issue.

At the Tevatron, only two production channels are important for the Standard Model Higgs boson.² In the moderate to high mass range, $140 \text{ GeV} \lesssim M_H \lesssim 200 \text{ GeV}$, the Higgs boson decays dominantly into W boson pairs (with one W state being possibly off mass-shell) [11], a description of the recent updates of the program can be found in [12], and the main production channel is the gluon-gluon fusion mechanism $gg \rightarrow H$ [13] which proceeds through heavy (mainly top and, to a lesser extent, bottom) quark triangular loops. The Higgs particle is then detected through the leptonic decays of the W bosons, $H \rightarrow WW^{(*)} \rightarrow \ell^+ \nu \ell^- \bar{\nu}$ with $\ell = e, \mu$, which exhibits different properties than the $p\bar{p} \rightarrow W^+W^- \rightarrow \ell\ell$ plus missing energy continuum background [14].

It is well known that the $gg \rightarrow H$ production process is subject to extremely large QCD radiative corrections [15–19], for a review of QCD effects in Higgs physics up to NLO see [20], [21–26]. In contrast, the electroweak radiative corrections are much smaller, being at the level of a few percent [27–32], i.e. as in the case of Higgs production at the LEP collider. For the corrections due to the strong interactions, the K -factor defined as the ratio of the higher order (HO) to the lowest order (LO) cross sections, consistently evaluated with the α_s value and the PDF sets at the chosen order,

$$K_{\text{HO}} = \sigma^{\text{HO}}|_{(\alpha_s^{\text{HO}}, \text{PDF}^{\text{HO}})} / \sigma^{\text{LO}}|_{(\alpha_s^{\text{LO}}, \text{PDF}^{\text{LO}})}, \quad (1.1)$$

is about a factor of two at next-to-leading order (NLO) [15–19] and about a factor of three at the next-to-next-to-leading order (NNLO) [21–23]. In fact, this exceptionally large K -factor is what allows a sensitivity on the Higgs boson at the Tevatron with the presently collected data. Nevertheless, the K -factor is so large that one may question the reliability of the perturbative series, despite of the fact that there seems to be kind of a convergence of the series as the NNLO correction is smaller than the NLO correction.³

¹An example of such a situation is the $p\bar{p} \rightarrow b\bar{b}$ production cross section that has been measured at the Tevatron (and elsewhere) and which was a factor of two to three larger than the theoretical prediction, before higher order effects and various uncertainties were included. For a review, see ref. [10] for instance.

²The CDF/D0 exclusion limits [8] have been obtained by considering a large variety of Higgs production and decay channels (36 and 54 exclusive final states for, respectively, the CDF and D0 collaborations) and combining them using artificial neural network techniques. However, as will be seen later, only a few channels play a significant role in practice.

³At LHC energies, the problem of the convergence of the perturbative series is less severe as the QCD K -factor is only ~ 1.7 at NLO and ~ 2 at NNLO in the relevant Higgs mass range.

In the low mass range, $M_H \lesssim 140$ GeV, the main Higgs decay channel is $H \rightarrow b\bar{b}$ [11, 12] and the gg fusion mechanism cannot be used anymore as the $gg \rightarrow H \rightarrow b\bar{b}$ signal is swamped by the huge QCD jet background. The Higgs particle has then to be detected through its associated production with a W boson $q\bar{q} \rightarrow WH$ [33] which leads to cleaner $\ell\nu b\bar{b}$ final states [34]. Additional topologies that can also be considered in this context are $q\bar{q} \rightarrow WH$ with $H \rightarrow WW^* \rightarrow \ell\ell\nu\nu$ or the twin production process $q\bar{q} \rightarrow ZH$ with the subsequent decays $H \rightarrow b\bar{b}$ and $Z \rightarrow \nu\bar{\nu}$ or $\ell^+\ell^-$. Other production/decay channels are expected to lead to very low rates and/or to be afflicted with too large QCD backgrounds.

At the Tevatron, the Higgs-strahlung processes $q\bar{q} \rightarrow VH$ with $V = W, Z$ receive only moderate higher order corrections: the QCD corrections increase the cross sections by about 40% at NLO [35–39] and 10% at NNLO [40], while the impact of the one-loop electroweak corrections is small, leading to a $\approx 5\%$ decrease of the cross sections [41]. Thus, in contrast to the gluon-gluon fusion process, the production cross sections in the Higgs-strahlung processes should be well under control.

In this paper, we first update the cross sections for these two main Higgs production channels at the Tevatron, including all known and relevant higher order QCD and electroweak corrections and using the latest MSTW2008 set of parton distribution functions [42, 43]. For the the $gg \rightarrow H$ process, this update has been performed in various recent analyses [25, 27] and, for instance, the normalized Higgs production cross sections used by the CDF/D0 collaborations in their combined analysis [8] are taken from these references. Such an update is lacking in the case of the Higgs-strahlung production channels $q\bar{q} \rightarrow VH$ and, for instance, the normalised cross sections used by the Tevatron experiments [8] are those given in ref. [45, 46] which make use of the old MRST2002 set of PDFs [47], a parametrisation that was approximate as it did not include the full set of evolved PDFs at NNLO. For completeness, we also update the cross sections for the two other single Higgs production channels at hadron colliders: the weak boson fusion $p\bar{p} \rightarrow qqH$ [48–53] and the associated production with top quark pairs $p\bar{p} \rightarrow t\bar{t}H$ [54–60]. These channels play only a minor role at the Tevatron but have also been included in the CDF/D0 analysis [8].

A second goal of the present paper is to investigate in a comprehensive way the impact of all possible sources of uncertainties on the total cross sections for the two main Higgs production channels. We first reanalyse the uncertainties from the unknown higher order effects, which are usually estimated by exploring the cross sections dependence on the renormalisation scale μ_R and the factorisation scale μ_F . In most recent analyses, the two scales are varied within a factor of two from a median scale which is considered as the most natural one. We show that this choice slightly underestimates the higher order effects and we use a criterion that allows a more reasonable estimate of the latter: the range of variation of the two scales μ_R and μ_F should be the one which allows the uncertainty band of the NLO cross section to match the central value of the cross section at the highest calculated order. In the case of $gg \rightarrow H$, for the uncertainty band of the NLO cross section to reach the central result of the NNLO cross section, a variation of μ_R and μ_F within a factor of ~ 3 from the central value $\mu_R = \mu_F = M_H$ is required. When the scales are varied within the latter range, one obtains an uncertainty on the NNLO cross section of $\approx 20\%$, which is slightly larger than what is usually assumed.

We then discuss the errors resulting from the folding of the partonic cross sections with the parton densities, considering not only the recent MSTW set of PDFs as in refs. [25–27], but also two other PDF sets that are available in the literature: CTEQ [61, 62] and ABKM [63, 64]. In the case of the cross section for the $gg \rightarrow H$ process at the Tevatron, we find that while the PDF uncertainties evaluated within the same scheme are moderate, as also shown in refs. [25–27], the central values of the cross sections obtained using the three schemes can be widely different. We show that it is only when the experimental as well as the theoretical errors on the strong coupling constant α_s are accounted for that one obtains results that are consistent when using the MSTW/CTEQ and ABKM schemes. As a result, the sum of the PDF+ $\Delta^{\text{exp}}\alpha_s$ and $\Delta^{\text{th}}\alpha_s$ uncertainties, that we evaluate using a set-up recently proposed by the MSTW collaboration to determine simultaneously the errors due to the PDFs and to α_s , is estimated to be at least a factor of two larger than what is generally assumed.

Finally, a third source of potential errors is considered in the gg fusion mechanism: the one resulting from the use of an effective field theory approach, in which the loop particle masses are assumed to be much larger than the Higgs boson mass, to evaluate the NNLO contributions. While this error is very small in the case of the top-quark contribution, it is at the percent level in the case of the b -quark loop contribution at NNLO QCD where the limit $M_H \ll m_b$ cannot be applied. This is also the case of the three-loop mixed QCD-electroweak radiative corrections that have obtained in the effective limit $M_H \ll M_W$, which lead to a few percent uncertainty. In addition, an uncertainty of about 1% originates from the freedom in the choice of the input b -quark mass in the Hgg amplitude. The total uncertainty in this context is thus not negligible and amounts to a few percent.

We then address the important issue of how to combine the theoretical errors originating from these different sources. Since using the usually adopted procedures of adding these errors either in quadrature, as is done by the experimental collaborations for instance, or linearly as is generally the case for theoretical errors, lead to either an underestimate or to an overestimate of the total error, we propose a procedure that is, in our opinion, more adequate. One first determines the maximal and minimal values of the cross sections obtained from the variation of the renormalisation and factorisation scales, and then estimate directly on these extrema cross sections the combined uncertainties due to the PDFs and to the experimental and theoretical errors on α_s . The other smaller theoretical uncertainties, such as those coming from the use of the effective approach in $gg \rightarrow H$, can be then added linearly to this scale, PDF and α_s combined error.

The main result of our paper is that, when adding all these uncertainties using our procedure, the total theoretical error on the production cross sections is much larger than what is often quoted in the literature. In particular, in the case of the most sensitive Higgs production channel at the Tevatron, $gg \rightarrow H \rightarrow \ell\ell\nu\nu$, the overall uncertainty on the NNLO total cross section is found to be of the order of $\approx -40\%$ and $\approx +50\%$. This is significantly larger than the uncertainty of $\approx \pm 10\%$ assumed in earlier studies and adopted in the CDF/D0 combined Higgs search analysis. As a result, we believe that the exclusion range given by the Tevatron experiments for the Higgs mass in the Standard Model, $162 \text{ GeV} \leq M_H \leq 166 \text{ GeV}$, should be reconsidered in the light of these results.

The rest of the paper is organised as follows. In the next section we outline our calculation of the Higgs production cross sections at the Tevatron in the gluon-gluon fusion and Higgs-strahlung processes. In section 3, we focus on the gluon-gluon fusion channel and evaluate the theoretical uncertainties on the cross section from scale variation, PDF and α_s uncertainties as well as from the use of the effective theory approach for the NNLO contributions. Section 4 addresses the same issues for the associated Higgs production channels. The various theoretical errors are summarized and combined in section 5 and their implications are discussed. A brief conclusion is given in section 6.

2 The production cross sections

In this section, we summarize the procedure which allows to obtain our updated central or “best” values of the total cross sections for Higgs production at the Tevatron in the Standard Model. We mainly discuss the two dominant channels, namely the gluon-gluon fusion and Higgs-strahlung, but for completeness, we mention the two other production channels: vector boson fusion and associated Higgs production with top quark pairs.

The production rate for the $gg \rightarrow H + X$ process, where X denotes the additional jets that appear at higher orders in QCD, is evaluated in the following way. The cross section up to NLO in QCD is calculated using the Fortran code HIGLU [65], the Fortran codes can be found in Michael Spira’s web page [66], which includes the complete set of radiative corrections at this order, taking into account the full dependence on the top and bottom quark masses [19]. The contribution of the NNLO corrections [21–23] is then implemented in this program using the analytical expressions given in ref. [22]. These corrections have been derived in an effective approach in which only the dominant top quark contribution is included in the infinite top quark mass limit but the cross section was rescaled by the exact m_t dependent Born cross section, an approximation which at NLO is accurate at the level of a few percent for Higgs masses below the $t\bar{t}$ kinematical threshold, $M_H \lesssim 300$ GeV [19, 20]. The dependence on the renormalisation scale μ_R and the factorisation scale μ_F of the partonic NNLO cross sections has been reconstructed from the scale independent expressions of ref. [22] using the fact that the full hadronic cross sections do not depend on them and the α_s running between the μ_F and μ_R scales.⁴ Nevertheless, for the central values of the cross sections which will be discussed in the present section, we adopt the usual scale choice $\mu_R = \mu_F = M_H$.

An important remark to be made at this stage is that we do not include the soft-gluon resummation contributions which, for the total cross section, have been calculated up to next-to-next-to-leading logarithm (NNLL) approximation and increase the production rate by ~ 10 – 15% at the Tevatron [24]. We also do not include the additional small contributions of the estimated contribution at N³LO [68] as well as those of soft terms beyond the NNLL approximation [69–72]. The reason is that these corrections are known only for

⁴The analytical expressions for the scale dependence have only been given in ref. [23] in the limit $\mu_F = \mu_R$ from which one can straightforwardly obtain the case $\mu_F \neq \mu_R$ (see also ref. [67]). We find agreement with this reference once the virtual+soft $gg \rightarrow H$ partonic cross sections given in the appendix are multiplied by the factor C_H given in eq. (2.7). We thank V. Ravindran for kindly clarifying this point to us.

the inclusive total cross section and not for the cross sections when experimental cuts are incorporated; this is also the case for the differential cross sections, see for instance [74–77], and many distributions that are used experimentally, which have been evaluated only at NNLO at most. This choice of ignoring the contributions beyond NNLO⁵ has also been adopted in ref. [26] in which the theoretical predictions have been confronted to the CDF/D0 results, the focus being the comparison between the distributions obtained from the matrix elements calculation with those given by the event generators and Monte-Carlo programs used by the experiments. Nevertheless, the NNLL result for the cross section can be very closely approached by evaluating the NNLO cross section at the renormalisation and factorisation scales $\mu_R = \mu_F = \frac{1}{2}M_H$ [24] as will be commented upon later.

For the electroweak part, we include the complete one-loop corrections to the $gg \rightarrow H$ amplitude which have been calculated in ref. [32] taking into account the full dependence on the top/bottom quark and the W/Z boson masses. These corrections are implemented in the so-called partial factorisation scheme in which the electroweak correction δ_{EW} is simply added to the QCD corrected cross section at NNLO, $\sigma^{\text{tot}} = \sigma^{\text{NNLO}} + \sigma^{\text{LO}}(1 + \delta_{EW})$. In the alternative complete factorization scheme discussed in ref. [32], the electroweak correction $1 + \delta_{EW}$ is multiplied by the fully QCD corrected cross section, $\sigma^{\text{tot}} = \sigma^{\text{NNLO}}(1 + \delta_{EW})$ and, thus, formally involves terms of $\mathcal{O}(\alpha_s^3\alpha)$ and $\mathcal{O}(\alpha_s^4\alpha)$ which have not been fully calculated. Since the QCD K -factor is large, $K_{\text{NNLO}} \approx 3$, the electroweak corrections might be overestimated by the same factor. We have also included the mixed QCD-electroweak corrections at NNLO due to light-quark loops [27]. These are only part of the three-loop $\mathcal{O}(\alpha\alpha_s)$ corrections and have been calculated in an effective approach that is valid only when $M_H \lesssim M_W$ and which cannot be easily extrapolated to M_H values above this threshold; this will be discussed in more details in the next section. In ref. [27], it has been pointed out that this procedure, i.e. adding the NLO full result and the mixed QCD-electroweak correction in the partial factorization scheme, is equivalent to simply including only the NLO electroweak correction in the complete factorisation scheme.

In the case of the $q\bar{q} \rightarrow WH$ and $q\bar{q} \rightarrow ZH$ associated Higgs production processes, we use the Fortran code V2HV [66] which evaluates the full cross sections at NLO in QCD. The NNLO QCD contributions to the cross sections [40], if the $gg \rightarrow ZH$ contribution (that does not appear in the case of WH production and is at the permille level at the Tevatron) is ignored, are the same as for the Drell-Yan process $p\bar{p} \rightarrow V^*$ with $V = W, Z$ [78] given in ref. [21, 79], once the scales and the invariant mass of the final state are properly adapted. These NNLO corrections, as well as the one-loop electroweak corrections evaluated in ref. [41], are incorporated in the program V2HV. The central scale adopted in this case is the invariant mass of the HV system, $\mu_R = \mu_F = M_{HV}$.

Folding the partonic cross sections with the most recent set of MSTW parton distribution functions [42, 43] and setting the renormalisation and factorisation scales at the most natural values discussed above, i.e. $\mu_R = \mu_F = M_H$ for $gg \rightarrow H$ and $\mu_R = \mu_F = M_{HV}$ for

⁵One could also advocate the fact that it is theoretically not very consistent to fold a resummed cross section with PDF sets which do not involve any resummation, as is the case for the presently available PDF sets which at at most at NNLO (although the effects of the resummation on the PDFs might be rather small in practice); see for instance the discussion given in ref. [73].

$q\bar{q} \rightarrow VH$, we obtain for the Tevatron energy $\sqrt{s} = 1.96$ TeV, the central values displayed in figure 1 for the Higgs production cross sections as a function of the Higgs mass. Note that we have corrected the numbers that we obtained in an earlier version of the paper for the $p\bar{p} \rightarrow HW$ cross section to include in the V2HV program the CKM matrix elements when folding the partonic $q\bar{q}' \rightarrow HW$ cross sections with the parton luminosities;⁶ this results in a decrease of the $p\bar{p} \rightarrow HW$ cross section by $\approx 4\%$. In addition, it recently appeared that including the combined HERA data and the Tevatron $W \rightarrow \ell\nu$ charge asymmetry data in the MSTW2008 PDF set [44] might lead to an increase of the $p\bar{p} \rightarrow (H+)Z/W$ cross sections by $\approx 3\%$; a small change in $\sigma(gg \rightarrow H)$ is also expected.

For the cross sections of the two sub-leading processes $qq \rightarrow V^*V^*qq \rightarrow Hqq$ and $q\bar{q}/gg \rightarrow t\bar{t}H$ that we also include in figure 1 for completeness, we have not entered into very sophisticated considerations. We have simply followed the procedure outlined in ref. [5] and used the public Fortran codes again given in ref. [66]. The vector boson total cross section is evaluated at NLO in QCD [52, 53] at a scale $\mu_R = \mu_F = Q_V$ (where Q_V is the momentum transfer at the gauge boson leg), while the presumably small electroweak corrections, known for the LHC [80], are omitted. In the case of associated $t\bar{t}H$ production, the LO cross section is evaluated at scales $\mu_R = \mu_F = \frac{1}{2}(M_H + 2m_t)$ but is multiplied by a factor $K \sim 0.8$ over the entire Higgs mass range to account for the bulk of the NLO QCD corrections [57–60]. In the latter case, we use the updated value $m_t = 173.1$ GeV for the top quark mass [81]. The only other update compared to the cross section values given in ref. [5] is thus the use of the recent MSTW set of PDFs.

In the case of the $gg \rightarrow H$ process, our results for the total cross sections are approximately 15% lower than those given in refs. [8, 25]. For instance, for $M_H = 160$ GeV, we obtain with our procedure a total $p\bar{p} \rightarrow H + X$ cross section of $\sigma^{\text{tot}} = 374$ fb, compared to the value $\sigma^{\text{tot}} = 439$ fb quoted in ref. [8, 25]. The difference is mainly due to the fact that we are working in the NNLO approximation in QCD rather than in the NNLL approximation. As already, mentioned and in accord with ref. [26], we believe that only the NNLO result should be considered as the production cross sections that are used experimentally include only NNLO effects (not to mention the fact that the K -factors for the cross sections with cuts are significantly smaller than the K -factors affecting the total inclusive cross section, as will be discussed in the next section). A small difference comes also from the different treatment of the electroweak radiative corrections (partial factorisation plus mixed QCD-electroweak contributions in our case versus complete factorisation in ref. [25]) and another one percent discrepancy can be attributed to the numerical uncertainties in the various integrations of the partonic sections.⁷

⁶We thank R. Harlander and Tom Zirke for pointing this problem to us.

⁷We have explicitly verified, using the program HRESUM [82] which led to the results of ref. [25], that our NNLO cross section is in excellent agreement with those available in the literature. In particular, for $M_H = 160$ GeV and scales $\mu_R = \mu_F = M_H$, one obtains $\sigma^{\text{NNLO}} = 380$ fb with HRESUM compared to $\sigma^{\text{NNLO}} = 374$ fb in our case; the 1.5% discrepancy being due to the different treatment of the electroweak corrections and the integration errors. Furthermore, setting the renormalisation and factorisation scales to $\mu_R = \mu_F = \frac{1}{2}M_H$, we find $\sigma^{\text{NNLO}} = 427$ fb which is in excellent agreement with the value $\sigma^{\text{NNLO}} = 434$ fb obtained in ref. [27] and with HRESUM, as well as the value in the NNLL approximation when the scales are set at their central values $\mu_R = \mu_F = M_H$. This gives us confidence that our implementation of the NNLO

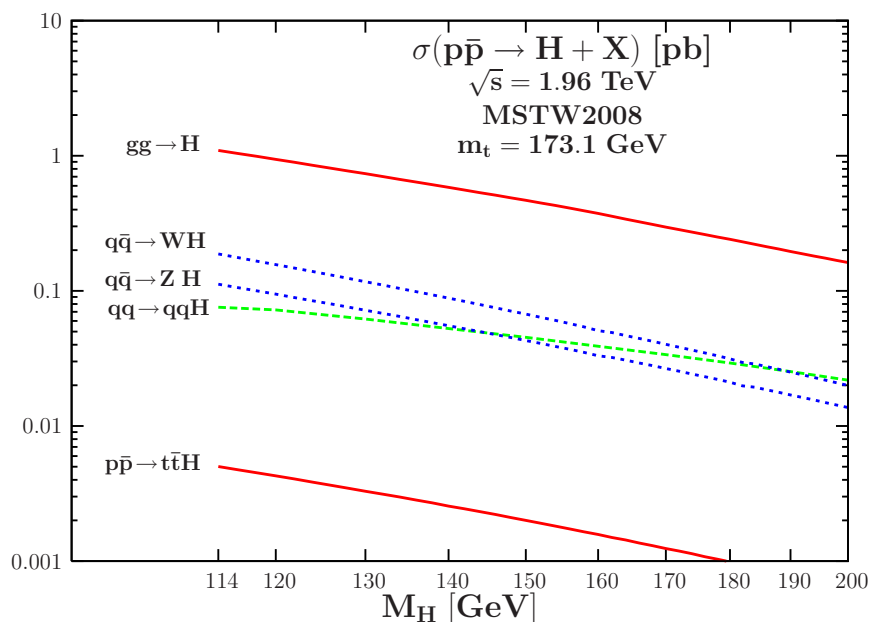


Figure 1. The total cross sections for Higgs production at the Tevatron as a function of the Higgs mass. The MSTW set of PDFs has been used and the higher order corrections are included as discussed in the text.

We should also note that for the Higgs mass value $M_H = 160$ GeV, we obtain $K \simeq 2.15$ for the QCD K -factor at NLO and $K \simeq 2.8$ at NNLO. These numbers are slightly different from those presented in ref. [26], $K \simeq 2.4$ and $K \simeq 3.3$, respectively. The reason is that the b -quark loop contribution, for which the K -factor at NLO is significantly smaller than the one for the top quark contribution [19] has been ignored for simplicity in the latter paper; this difference will be discussed in section 3.2.

In the case of Higgs-strahlung from W and Z bosons, the central values of the cross sections that we obtain are comparable to those given in ref. [8, 45, 46], with at most a $\sim 2\%$ decrease in the low Higgs mass range, $M_H \lesssim 140$ GeV. The reason is that the quark and antiquark densities, which are the most relevant in these processes and are more under control than the gluon densities, are approximately the same in the new MSTW2008 and old MRST2002 sets of PDFs (although the updated set includes a new fit to run II Tevatron and HERA inclusive jet data). We should note that for $M_H = 115$ GeV for which the production cross sections are the largest, $\sigma^{\text{WH}} = 175$ fb and $\sigma^{\text{ZH}} = 104$ fb, the QCD K -factors are ~ 1.2 (1.3) at NLO (NNLO), while the electroweak corrections decrease the LO cross sections by $\approx -5\%$. The correcting factors do not change significantly for increasing M_H values for the Higgs mass range relevant at the Tevatron.

Finally, the cross sections for the vector boson fusion channel in which the recent MSTW set of PDFs is used agree well with those given in refs. [8, 83], values of the cross contributions in the NLO code HIGLU, including the scale dependence, is correct.

sections can be found at [84]. In the case of the $t\bar{t}H$ associated production process, a small difference is observed compared to ref. [5] in which the 2005 $m_t = 178$ GeV value is used: we have a few percent increase of the rate due the presently smaller m_t value which provides more phase space for the process, overcompensating the decrease due to the smaller top-quark Yukawa coupling.

Before closing this section, let us make a few remarks on the Higgs decay branching ratios and on the rates for the various individual channels that are used to detect the Higgs signal at the Tevatron. For the the Higgs decays, one should use the latest version (3.51) of the program HDECAY [11, 12] in which the important radiative corrections to the $H \rightarrow WW$ decays [85, 86] have been recently implemented. Choosing the option which allows for the Higgs decays into double off-shell gauge bosons, $H \rightarrow V^*V^*$, which provides the best approximation⁸ and using the updated input parameters $\alpha_s(M_Z) = 0.1172$, $m_t = 173.1$ GeV and $m_b^{\text{pole}} = 4.6$ GeV, one obtains the results shown in table 1 for the three dominant decay channels in the mass range relevant at the Tevatron, $H \rightarrow W^*W^*, b\bar{b}$ and $\tau^+\tau^-$. These results are slightly different from those given in ref. [8]. In particular, the $H \rightarrow W^*W^*$ rate that we obtain is a few percent larger for Higgs masses below ~ 170 GeV.

In the interesting range $160 \text{ GeV} \leq M_H \leq 170$ for which the Tevatron experiments are most sensitive, one sees that the branching ratio for the $H \rightarrow WW$ is largely dominant, being above 90%. In addition, in this mass range, the $gg \rightarrow H$ cross section is one order of magnitude larger than the cross sections for the $q\bar{q} \rightarrow WH, ZH$ and $qq \rightarrow qqH$ processes as for $M_H \sim 160$ GeV for instance, one has $\sigma(gg \rightarrow H) = 374$ fb compared to $\sigma(WH) \simeq 50$ fb, $\sigma(ZH) \simeq 30$ fb and $\sigma(qqH) \simeq 40$ fb. Thus, the channel $gg \rightarrow H \rightarrow W^*W^*$ represents, even before selection cuts are applied, the bulk of the events leading to $\ell\ell\nu\nu + X$ final states, where here X stands for additional jets or leptons coming from W, Z decays as well as for jets due to the higher order corrections to the $gg \rightarrow H$ process. In the lower Higgs mass range, $M_H \lesssim 150$ GeV, all the production channels above, with the exception of the vector boson $qq \rightarrow qqH$ channel which can be selected using specific kinematical cuts, should be taken into account but with the process $q\bar{q} \rightarrow WH \rightarrow \ell\nu b\bar{b}$ being dominant for $M_H \lesssim 130$ GeV. This justifies the fact that we concentrate on the gluon-gluon fusion and Higgs-strahlung production channels in this paper.

3 Theoretical uncertainties in gluon-gluon fusion

3.1 The scale uncertainty and higher order effects

It has become customary to estimate the effects of the unknown (yet uncalculated) higher order contributions to production cross sections and distributions at hadron colliders by studying the variation of these observables, evaluated at the highest known perturbative order, with the renormalisation scale μ_R which defines the strong coupling constant α_s and the factorisation scale μ_F at which one performs the matching between the perturbative

⁸The options in HDECAY where one or two vector bosons are allowed to be on mass-shell do not give precise results. In addition, in earlier versions, there was an interpolation which smoothed the transition from below to above the kinematical threshold, $M_H \approx 2M_W$, i.e. right in the most interesting Higgs mass region at the Tevatron. The option of both gauge bosons being off mass-shell should be therefore used.

M_H (GeV)	$BR(H \rightarrow W^*W^*)$	$BR(H \rightarrow b\bar{b})$	$BR(H \rightarrow \tau^+\tau^-)$
115	8.311	73.02	7.328
120	13.72	67.53	6.832
125	20.91	60.44	6.161
130	29.63	52.02	5.342
135	39.35	42.83	4.429
140	49.45	33.56	3.493
145	59.43	24.81	2.599
150	69.17	16.94	1.785
155	79.11	10.60	1.060
160	90.56	3.786	0.404
165	95.94	1.303	0.140
170	96.41	0.863	0.093
175	95.82	0.669	0.072
180	93.26	0.540	0.058
185	84.51	0.419	0.046
190	78.71	0.343	0.038
195	75.89	0.294	0.033
200	74.26	0.259	0.029

Table 1. The branching ratios (in %) of the main decay channels of the Standard Model Higgs boson using the latest version of the program HDECAY [11, 12].

calculation of the matrix elements and the non-perturbative part which resides in the parton distribution functions. The dependence of the cross sections and distributions on these two scales is in principle unphysical: when all orders of the perturbative series are summed, the observables should be scale independent. This scale dependence appears because the perturbative series are truncated, as only its few first orders are evaluated in practice, and

can thus serve as a guess of the impact of the higher order contributions.

Starting from a median scale μ_0 which, with an educated guess, is considered as the most “natural” scale of the process and absorbs potentially large logarithmic corrections, the current convention is to vary these two scales within the range

$$\mu_0/\kappa \leq \mu_R, \mu_F \leq \kappa\mu_0. \tag{3.1}$$

with the constant factor κ to be determined. One then uses the following equations to calculate the deviation of, for instance, a cross section $\sigma(\mu_R, \mu_F)$ from the central value evaluated at scales $\mu_R = \mu_F = \mu_0$,

$$\begin{aligned} \Delta\sigma_\mu^+ &= \max_{(\mu_R, \mu_F)} \sigma(\mu_R, \mu_F) - \sigma(\mu_R = \mu_F = \mu_0), \\ \Delta\sigma_\mu^- &= \sigma(\mu_R = \mu_F = \mu_0) - \min_{(\mu_R, \mu_F)} \sigma(\mu_R, \mu_F). \end{aligned} \tag{3.2}$$

This procedure is by no means a true measure of the higher order effects and should be viewed only as providing a guess of the lower limit on the scale uncertainty. The variation of the scales in the range of eq. (3.1) can be individual with μ_R and μ_F varying independently in this domain, with possibly some constraints such as $1/\kappa \leq \mu_R/\mu_F \leq \kappa$ in order not to generate “artificially large logarithms”, or collective when, for instance, keeping one of the two scales fixed, say to μ_0 , and vary the other scale in the chosen domain. Another possibility which is often adopted, is to equate the two scales, $\mu_0/\kappa \leq \mu_R = \mu_F \leq \kappa\mu_0$, a procedure that is possibly more consistent as most PDF sets are determined and evolved according to $\mu_R = \mu_F$, but which has no theoretical ground as the two scales enter different parts of the calculation (renormalisation versus factorisation).

In addition, there is a freedom in the choice of the variation domain for a given process and, hence, of the constant factor κ . This choice is again rather subjective: depending on whether one is optimistic or pessimistic, i.e. believes or not that the higher order corrections to the process are under control, it can range from $\kappa=2$ to much higher values.

In most recent analyses of production cross sections at hadron colliders, a kind of consensus has emerged and the domain,

$$\frac{1}{2}\mu_0 \leq \mu_R, \mu_F \leq 2\mu_0, \quad \frac{1}{2} \leq \mu_R/\mu_F \leq 2, \tag{3.3}$$

has been generally adopted for the scale variation. A first remark is that the condition $\frac{1}{2} \leq \mu_R/\mu_F \leq 2$ to avoid the appearance of large logarithms might seem too restrictive: after all, these possible large logarithms can be viewed as nothing else than the logarithms involving the scales and if they are large, it is simply a reflection of a large scale dependence. A second remark is that in the case of processes in which the calculated higher order contributions are small to moderate and the perturbative series appears to be well behaved,⁹ the choice of such a narrow domain for the scale variation with $\kappa = 2$, appears reasonable. This, however,

⁹This is indeed the case for some important production processes at the Tevatron, such as the Drell-Yan process $p\bar{p} \rightarrow V$ [79, 87, 88], weak boson pair production [89–93] and even top quark pair production [94–96] once the central scale is taken to be $\mu_0 = m_t$, which have moderate QCD corrections.

might not be true in processes in which the calculated radiative corrections turn out to be extremely large. As the higher order contributions might also be significant in this case, the variation domain of the renormalisation and factorisation scales should be extended and a range with a factor κ substantially larger than two seems more appropriate.¹⁰

In the case of the $gg \rightarrow H$ production process, the most natural value for the median scale is the Higgs mass itself, $\mu_0 = M_H$, and the effects of the higher order contributions to the cross section is again usually estimated by varying μ_R and μ_F as in eq. (3.3), i.e. with the choice $\frac{1}{\kappa} \leq \mu_R/\mu_F \leq \kappa$ and $\kappa = 2$. At the Tevatron, one obtains a variation of approximately $\pm 15\%$ of the NNLO cross section with this specific choice [21, 22] and the uncertainty drops to the level of $\approx \pm 10\%$ in the NNLL approximation. Note that in some analyses, see e.g. ref. [27], the central scale $\mu_0 = \frac{1}{2}M_H$ is chosen for the NNLO cross section to mimic the soft-gluon resummation at NNLL [24], and the variation domain $\frac{1}{4}M_H \leq \mu_R = \mu_F \leq M_H$ is then adopted, leading also to a $\approx 15\%$ uncertainty

Nevertheless, as the K -factor is extraordinarily large in the $gg \rightarrow H$ process, $K_{\text{NNLO}} \approx 3$, the domain of eq. (3.3) for the scale variation seems too narrow. If this scale domain was chosen for the LO cross section for instance, the maximal value of $\sigma(gg \rightarrow H)$ at LO would have never caught, and by far, the value of $\sigma(gg \rightarrow H)$ at NNLO, as it should be the case if the uncertainty band with $\kappa = 2$ were indeed the correct “measure” of the higher order effects. Only for a much larger value of κ that this would have been the case.

Here, we will use a criterion which allows an empirical evaluation of the effects of the still unknown high orders of the perturbative series and, hence, the choice of the variation domain of the factorisation and renormalisation scales in a production cross section (or distribution). This is done in two steps:

- i) The domain of scale variation, $\mu_0/\kappa \leq \mu_R, \mu_F \leq \kappa\mu_0$, is derived by calculating the factor κ which allows the uncertainty band of the lower order cross section resulting from the variation of μ_R and μ_F , to reach the central value (i.e. with μ_R and μ_F set to μ_0), of the cross section that has been obtained at the higher perturbative order.
- ii) The scale uncertainty on the cross section at the higher perturbative order is then taken to be the band obtained for a variation of the scales μ_R and μ_F within the same range and, hence, using the same κ value.

In the case of the $gg \rightarrow H$ process at the Tevatron, if the lower order cross section is taken to be simply σ^{LO} and the higher order one σ^{NNLO} , this is exemplified in the

¹⁰This would have been the case, for instance, in top-quark pair production at the Tevatron if the central scale were fixed to the more “natural” value $\mu_0 = 2m_t$ (instead of the value $\mu_0 = m_t$ usually taken [94–96]) and a scale variation within $\frac{1}{4}M_H \leq \mu_R, \mu_F \leq 4M_H$ were adopted. Another well known example is Higgs production in association with b -quark pairs in which the cross section can be determined by evaluating the mechanism $gg/q\bar{q} \rightarrow b\bar{b}H$ [97] or $b\bar{b}$ annihilation, $b\bar{b} \rightarrow H$ [98–100]. The two calculations performed at NLO for the former process and NNLO for the later one, are consistent only if the central scale is taken to be $\mu_0 \approx \frac{1}{4}M_H$ instead of the more “natural” value $\mu_0 \approx M_H$ [101]. Again, without prior knowledge of the higher order corrections, it would have been wiser, if the central scale $\mu_0 = M_H$ had been adopted, to assume a wide domain, e.g. $\frac{1}{4}M_H \leq \mu_R, \mu_F \leq 4M_H$, for the scale variation. Note that even for the scale choice $\mu_0 \approx \frac{1}{4}M_H$, the K -factor for the $gg \rightarrow b\bar{b}H$ process remains very large, $K_{\text{NLO}} \approx 2$ at the Tevatron. In addition, here, it is the factorisation scale μ_F which generates the large contributions $\propto \ln(\mu_F^2/m_b^2)$ and not the renormalisation scale which can be thus kept at the initial value $\mu_R \approx M_H$.

left-hand side of figure 2. The figure shows the uncertainty band of σ^{LO} resulting from a scale variation in the domain $M_H/\kappa \leq \mu_R, \mu_F \leq \kappa M_H$ with $\kappa = 2, 3, 4, 5$, which is then compared to σ^{NNLO} evaluated at the central scale $\mu_R = \mu_F = M_H$. One first observes that, as expected, the uncertainty bands are larger with increasing values of κ .

The important observation that one can draw from this figure is that it is only for $\kappa=5$, i.e. a variation of the scales in a range that is much wider than the one given in eq. (3.3) that the uncertainty band of the LO cross section becomes very close to (and still does not yet reach for low Higgs mass values) the curve giving the NNLO result. Thus, as the scale uncertainty band of $\sigma^{\text{LO}}(gg \rightarrow H)$ is supposed to provide an estimate of the resulting cross section at NNLO and beyond, the range within which the two scales μ_R and μ_F should be varied must be significantly larger than $\frac{1}{2}M_H \leq \mu_R, \mu_F \leq 2M_H$. One should not impose a restriction on μ_R/μ_F and consider at least the range¹¹ $\frac{1}{5}M_H \leq \mu_R, \mu_F \leq 5M_H$.

Nevertheless, one might be rightfully reluctant to use σ^{LO} as a starting point for estimating the higher order effects, as it is well known that it is only after including at least the next-order QCD corrections that a cross section is somewhat stabilized and, in the particular case of the $gg \rightarrow H$ process, the LO cross section does not describe correctly the kinematics as, for instance, the Higgs transverse momentum is zero at this order. We thus explore also the scale variation of the NLO cross section σ^{NLO} instead of that of σ^{LO} and compare the resulting uncertainty band to the central value of the cross section again at NNLO (we refrain here from adding the $\sim 15\%$ contribution at NNLL as well as those arising from higher order corrections, such as the estimated N³LO correction [68]).

The scale uncertainty bands of σ^{NLO} are shown in the right-hand side of figure 2 as a function of M_H again for scale variation in the domain $M_H/\kappa \leq \mu_R, \mu_F \leq \kappa M_H$ with $\kappa = 2, 3$ and 4, and are compared to σ^{NNLO} evaluated at the central scale $\mu_R = \mu_F = M_H$. One can see that, in this case, the uncertainty band for σ^{NLO} shortly falls to reach σ^{NNLO} for $\kappa=2$ and only for $\kappa=3$ that this indeed occurs in the entire M_H range.

Thus, to attain the NNLO values of the $gg \rightarrow H$ cross section at the Tevatron with the scale variation of the NLO cross section, when both cross sections are taken at the central scale choice¹² $\mu_R = \mu_F = \mu_0 = M_H$, one needs to chose the values $\kappa = 3$, and hence

¹¹Note that, in this case, the maximal LO cross section is obtained for small values of the two scales μ_R and μ_F . In fact, if the central value for the scales had been chosen to be $\mu_F = \mu_R = \frac{1}{5}M_H$ for instance, one would have obtained at LO, NLO and NNLO a cross section $\sigma^{\text{LO}} = 360$ fb, $\sigma^{\text{NLO}} = 526$ fb and $\sigma^{\text{NNLO}} = 475$ fb for the Higgs mass value $M_H = 160$ GeV. The increase of the LO cross section by a factor of ≈ 2.8 , compared to the case $\mu_F = \mu_R = M_H$ where one has $\sigma^{\text{LO}} = 129$ fb for the chosen M_H value, has absorbed the bulk of the higher order corrections. This allows a good convergence of the perturbative series as in this case one has $K_{\text{NLO}} = 1.46$ and $K_{\text{NNLO}} = 1.32$, which seems to stabilize the cross section between the NLO and NNLO values. This nice picture is not spoiled by soft-gluon resummation which leads for such a scale to $\sigma^{\text{NNLL}} = 459$ fb and, hence, the K -factor turns to $K_{\text{NNLL}} = 1.28$ which is only a few percent lower than K_{NNLO} . Thus, it might have been worth to choose $\mu_0 = \frac{1}{5}M_H$ as the central scale from the very beginning, although this particular value does not look very “natural” a priori. We also point out the fact that the choice $\mu_0 = \frac{1}{5}M_H$ for the central scale, provides an example of a reduction of the cross section when higher order contributions are taken into account as $K_{\text{NNLL}} < K_{\text{NNLO}} < K_{\text{NLO}}$.

¹²We note that one could choose the central scale value $\mu_0 = \frac{1}{2}M_H$ [27], instead of $\mu_0 = M_H$, which seems to better describe the essential features of the kinematics of the process, and in this case, a variation within a factor of two from this central value would have been sufficient for σ^{NLO} to attain σ^{NNLO} . We thank Babis Anastasiou for a discussion on this point.

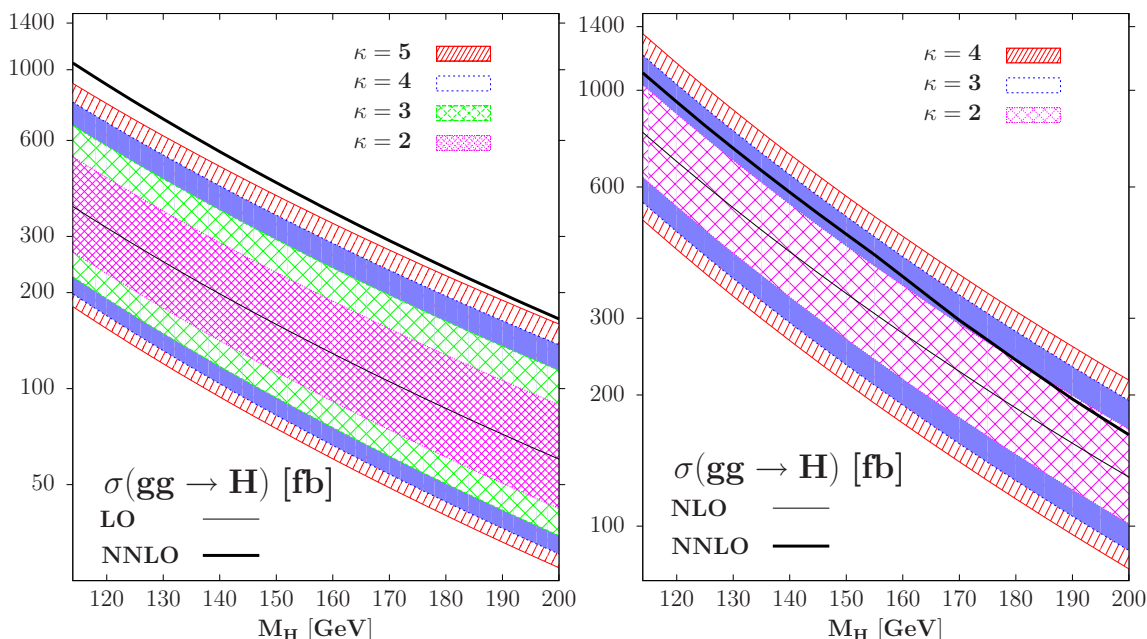


Figure 2. Left: the scale dependence of $\sigma^{\text{LO}}(\text{gg} \rightarrow \text{H})$ at the Tevatron as a function of M_H for scale variations $M_H/\kappa \leq \mu_R, \mu_F \leq \kappa M_H$ with $\kappa = 2, 3, 4$ and 5 compared to σ^{NNLO} for the central scale choice $\mu_R = \mu_F = M_H$. Right: the scale dependence of $\sigma^{\text{NLO}}(\text{gg} \rightarrow \text{H})$ at the Tevatron as a function of M_H for variations $M_H/\kappa \leq \mu_R, \mu_F \leq \kappa M_H$ with $\kappa = 2, 3$ and 4 compared to σ^{NNLO} evaluated at the central scale $\mu_R = \mu_F = M_H$.

a domain of scale variation that is wider than that given in eq. (3.3). This choice of the domains of scale variation might seem somewhat conservative at first sight. However, we emphasise again that in view of the huge QCD corrections which affect the cross section of this particular process, and which almost jeopardize the convergence of the perturbative series, this choice appears to be justified. In fact, this scale choice is not so unusual and in refs. [22–24, 102–104] for instance, scale variation domains comparable to those discussed here, and sometimes even wider, have been used for illustration.

Thus, in our analysis, rather than taking the usual choice for the scale domain of variation with $\kappa = 2$ given in eq. (3.3), we will adopt the slightly more conservative possibility given by the wider variation domain¹³

$$\frac{1}{3}M_H \leq \mu_R, \mu_F \leq 3M_H. \quad (3.4)$$

¹³One might argue that since in the case of $\sigma(\text{gg} \rightarrow \text{H})$, the NLO and NNLO contributions are both positive and increase the LO rate, one should expect a positive contribution from higher orders (as is the case for the re-summed NNLL contribution) and, thus, varying the scales using $\kappa = 2$ is more conservative, as the obtained maximal value of the cross section would be smaller than the value that one would obtain for e.g. $\kappa = 3$. However, one should not assume that the higher order contributions always increase the lower order cross sections. Indeed, as already mentioned, had we taken the central scales at $\mu_R = \mu_F = \frac{1}{5}M_H$, the NNLO (and even NNLL) corrections would have reduced the total cross section evaluated at NLO. Hence, the higher order contributions to $\sigma(\text{gg} \rightarrow \text{H})$ could well be negative beyond NNLO and could bring the value of the production cross section close to the lower range of the scale uncertainty band of σ^{NNLO} . Another good counter-example of a cross section that is reduced by the higher order contributions is the process of associated Higgs production with top quark pairs at the Tevatron where the NLO QCD corrections decrease the LO cross section by $\sim 20\%$ [57–60] once the central scale is chosen to be $\mu_0 = \frac{1}{2}(2m_t + M_H)$.

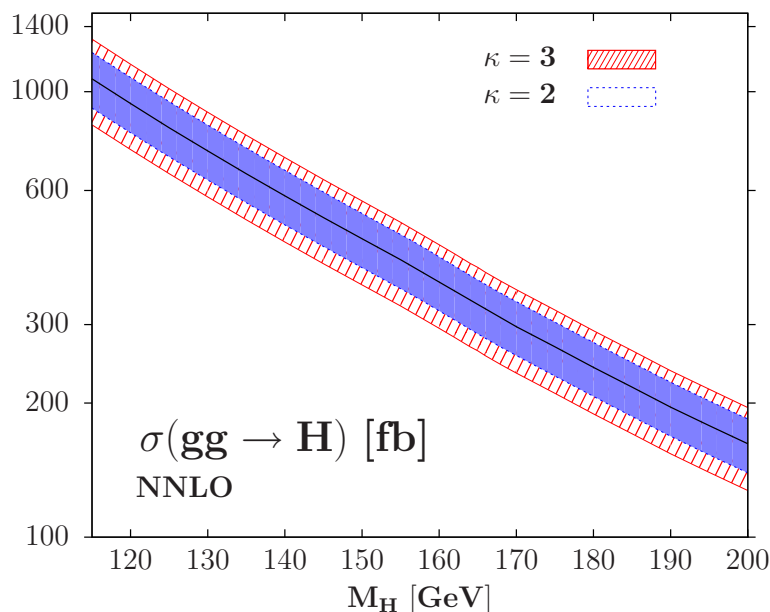


Figure 3. The uncertainty bands of the NNLO $gg \rightarrow H$ cross section at the Tevatron as a function of M_H for scale variation in the domains $\frac{1}{3}M_H \leq \mu_R, \mu_F \leq 3M_H$ and $\frac{1}{2}M_H \leq \mu_R, \mu_F \leq 2M_H$.

Having made this choice for the factor κ , one can turn to the estimate of the higher order effects of $\sigma(gg \rightarrow H)$ evaluated at the highest perturbative order that we take to be NNLO, ignoring again the known small contributions beyond this fixed order.

The uncertainty bands resulting from scale variation of $\sigma^{\text{NNLO}}(gg \rightarrow H)$ at NNLO in the domains given by eqs. (3.3) and (3.4) are shown in figure 3 as a function of M_H . As expected, the scale uncertainty is slightly larger for $\kappa = 3$ than for $\kappa = 2$. For instance, for $M_H = 160$ GeV, the NNLO cross section varies by up to $\sim \pm 21\%$ from its central value, $\sigma^{\text{NNLO}} = 374 \pm 80$ fb, compared to the $\approx \pm 14\%$ variation that one obtains for $\kappa = 2$, $\sigma^{\text{NNLO}} = 374 \pm 52$ fb. The minimal cross section is obtained for the largest values of the two scales, $\mu_F = \mu_R = \kappa M_H$, while the maximal value is obtained for the lowest value of the renormalisation scale, $\mu_R = \frac{1}{\kappa} M_H$, almost independently of the factorisation scale μ_F , but with a slight preference for the lowest μ_F values, $\mu_F = \frac{1}{\kappa} M_H$.

We should note that the $\approx 10\%$ scale uncertainty obtained in ref. [25] and adopted by the CDF/D0 collaborations [8] is even smaller than the ones discussed above. The reason is that it is the resummed NNLL cross section, again with $\kappa=2$ and $\frac{1}{2} \leq \mu_R/\mu_F \leq 2$, that was considered, and the scale variation of σ^{NNLL} is reduced compared to that of σ^{NNLO} in this case. As one might wonder if this milder dependence also occurs for our adopted κ value, we have explored the scale variation of σ^{NNLL} in the case of $\kappa = 3$, without the restriction $\frac{1}{3} \leq \mu_R/\mu_F \leq 3$. Using again the program HRESUM [82], we find that the difference between the maximal value of the NNLL cross section, obtained for $\mu_R \approx M_H$ and $\mu_F \approx 3M_H$, and its minimal value, obtained for $\mu_F \approx \frac{1}{3}M_H$ and $\mu_R \approx 3M_H$, is as large as in the NNLO case (this is also true for larger κ values). The maximal decrease and maximal increase of σ^{NNLL}

from the central value are still of about $\pm 20\%$ in this case. Hence, the relative stability of the NNLL cross section against scale variation, compared to the NNLO case, occurs only for $\kappa = 2$ and may appear as accidentally due to a restrictive choice of the variation domain. However, if the additional constraint $1/\kappa \leq \mu_F/\mu_R \leq \kappa$ is implemented, the situation would improve in the NNLL case, as the possibility $\mu_F \approx \frac{1}{\kappa}M_H$ and $\mu_R \approx \kappa M_H$ which minimizes σ^{NNLL} would be absent and the scale variation reduced. Nevertheless, even in this case, the variation of σ^{NNLL} for $\kappa = 3$ is of the order of $\approx \pm 15\%$ and, hence, the scale uncertainty is larger than what is obtained in the domain of eq. (3.3).

Finally, another reason for a more conservative choice of the scale variation domain for σ^{NNLO} , beyond the minimal $\frac{1}{2}M_H \leq \mu_R, \mu_F \leq 2M_H$ range, is that it is well known that the QCD corrections are significantly larger for the total inclusive cross section than for that on which basic selection cuts are applied; see e.g. ref. [74–77]. This can be seen from the recent analysis of ref. [26], in which the higher order corrections to the inclusive cross section for the main Tevatron Higgs signal, $gg \rightarrow H \rightarrow \ell\nu\nu$, have been compared to those affecting the cross section when selection cuts, that are very similar to those adopted by the CDF and D0 collaborations in their analysis (namely lepton selection and isolation, a minimum requirement for the missing transverse energy due to the neutrinos, and a veto on hard jets to suppress the $t\bar{t}$ background), are applied. The output of this study is that the K -factor for the cross section after cuts is $\sim 20\text{--}30\%$ smaller than the K -factor for the inclusive total cross section (albeit with a reduced scale dependence). For instance, one has $K_{\text{cuts}}^{\text{NNLO}} = 2.6$ and $K_{\text{total}}^{\text{NNLO}} = 3.3$ for $M_H = 160$ GeV and scales set to $\mu_F = \mu_R = M_H$.

Naively, one would expect that this $\sim 20\text{--}30\%$ reduction of the higher order QCD corrections when selection cuts are applied, if not implemented from the very beginning in the normalisation of the cross section after cuts that is actually used by the experiments (which would then reduce the acceptance of the signal events, defined as $\sigma_{\text{cuts}}^{\text{NNLO}}/\sigma_{\text{total}}^{\text{NNLO}}$), to be at least reflected in the scale variation of the inclusive cross section and, thus, accounted for in the theoretical uncertainty. This would be partly the case for scale variation within a factor $\kappa = 3$ from the central scale, which leads to a maximal reduction of the $gg \rightarrow H \rightarrow \ell\nu\nu$ cross section by about 20%, but not with the choice $\kappa = 2$ made in refs. [8] which would have led to a possible reduction of the cross section by $\approx 10\%$ only.¹⁴

3.2 Uncertainties due to the effective approach

While both the QCD and electroweak radiative corrections to the process $gg \rightarrow H$ have been calculated exactly at NLO, i.e taking into account the finite mass of the particles running in the loops, these corrections are derived at NNLO only in an effective approach in which the loop particles are assumed to be very massive, $m \gg M_H$, and integrated out. At the Born level, taking into account only the dominant contribution of the top quark loop and working in the limit $m_t \rightarrow \infty$ provides an approximation [19, 20] that is only good at the 10% level for Higgs masses below the $t\bar{t}$ kinematical threshold, $M_H \lesssim 350$ GeV. The difference from the exact result is mainly due to the absence of the contribution of

¹⁴The discussion is, however, more involved as one has to consider the efficiencies obtained with the NNLO calculation compared to that obtained with the Monte-Carlo used by the experiments; see ref. [26].

the b -quark loop: although the b -quark mass is small, the $gg \rightarrow H$ amplitude exhibits a dependence $\propto m_b^2/M_H^2 \times \log^2(m_b^2/M_H^2)$ which, for relatively low values of the Higgs mass, generates a non-negligible contribution that interferes destructively with the dominant top-quark loop contribution. In turn, when considering only the top quark loop in the Hgg amplitude, the approximation $m_t \rightarrow \infty$ is extremely good for Higgs masses below $2m_t$, compared to the amplitude with the exact top quark mass dependence.

In the NLO approximation for the QCD radiative corrections, it has been shown [19] that the exact K -factor when the full dependence on the top and bottom quark masses is taken into account, $K_{\text{NLO}}^{\text{exact}}$, is smaller than the K factor obtained in the approximation in which only the top quark contribution is included and the asymptotic limit $m_t \rightarrow \infty$ is taken, $K_{\text{NLO}}^{m_t \rightarrow \infty}$. The reason is that when only the b -quark loop contribution is considered in the Hgg amplitude (as in the case of supersymmetric theories in which the b -quark Yukawa coupling is strongly enhanced compared to its Standard Model value, for a review see [105]), the K -factor for the $gg \rightarrow H$ cross section at the Tevatron is about $K \sim 1.2$ to 1.5 , instead of $K \sim 2.4$ when only the top quark is included in the loop. The approximation of infinite loop particle mass significantly improves when the full t, b mass dependence is included in the LO order cross section and $\sigma_{\text{NLO}}^{m_t \rightarrow \infty} = K_{\text{NLO}}^{m_t \rightarrow \infty} \times \sigma_{\text{LO}}(m_t, m_b)$ gets closer to the cross section $\sigma_{\text{NLO}}^{\text{exact}}$ in which the exact m_t, m_b dependence is taken into account. In fact, this approximation works at the 10% level even beyond the $M_H \gtrsim 2m_t$ threshold where the Hgg amplitude develops imaginary parts that do not appear in the effective approach.

The difference between $\sigma_{\text{NLO}}^{\text{exact}}$ and $\sigma_{\text{NLO}}^{m_t \rightarrow \infty}$ at Tevatron energies is shown in figure 4 as a function of the Higgs mass and, as one can see, there is a few percent discrepancy between the two cross sections. As mentioned previously, in the Higgs mass range $115 \text{ GeV} \lesssim M_H \lesssim 200 \text{ GeV}$ relevant at Tevatron energies, this difference is solely due to the absence of the b -quark loop contribution and its interference with the top quark loop in the Hgg amplitude and not to the fact that the limit $m_t \gg M_H$ is taken.

At NNLO, because of the complexity of the calculation, only the result in the effective approach in which the loop particle masses are assumed to be infinite is available. In the case of the NNLO QCD corrections [21–23], the b -quark loop contribution and its interference with the contribution of t -quark loop is therefore missing. Since the NNLO correction increases the cross section by $\sim 30\%$, one might wonder if this missing piece does not lead to an overestimate of the total K -factor. We will assume that it might be indeed the case and assign an error on the NNLO QCD result which is approximately the difference between the exact result $\sigma_{\text{NLO}}^{\text{exact}}$ and the approximate result $\sigma_{\text{NLO}}^{m_t \rightarrow \infty}$ obtained at NLO and shown in figure 4, but rescaled with the relative magnitude of the K -factors that one obtains at NLO and NNLO, i.e. $K_{\text{NLO}}^{m_t \rightarrow \infty}/K_{\text{NNLO}}^{m_t \rightarrow \infty}$. This leads to an uncertainty on the NNLO cross section which ranges from $\sim \pm 2\%$ for low Higgs values $M_H \sim 120 \text{ GeV}$ at which the b -quark loop contribution is significant at LO, to the level of $\sim \pm 1\%$ for Higgs masses above $M_H \sim 180 \text{ GeV}$ for which the b -quark loop contribution is much smaller.

In addition one should assign to the b -quark contribution an error originating from the freedom in choosing the input value of the b -quark mass in the loop amplitude and the

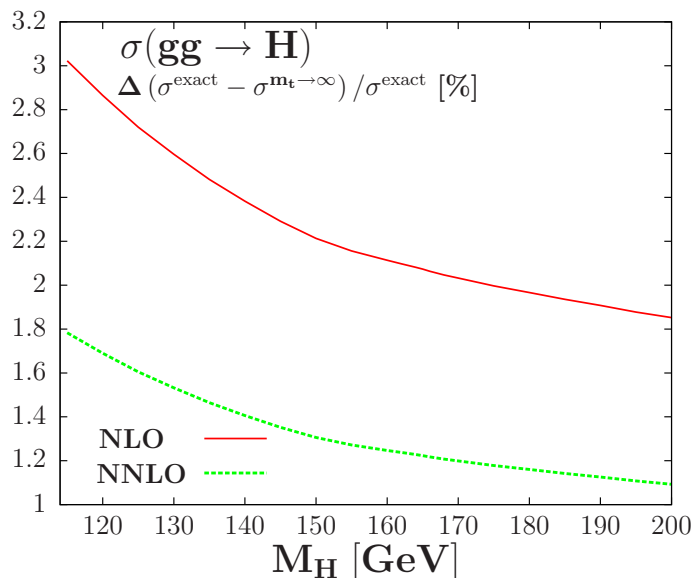


Figure 4. Relative difference (in %) at Tevatron energies and as a function of M_H between the exact NLO and NNLO $gg \rightarrow H$ cross sections $\sigma_{\text{NLO/NNLO}}^{\text{exact}}$ and the cross section in the effective approach with an infinite top quark mass $\sigma_{\text{NLO/NNLO}}^{m_t \rightarrow \infty}$.

scheme in which it is defined.¹⁵ Indeed, besides the difference obtained when using the b -quark pole mass, $M_b^{\text{pole}} \approx 4.7 \text{ GeV}$, as is done here or the running $\overline{\text{MS}}$ mass evaluated at the scale of the b -quark mass, $\overline{m}_b^{\text{MS}}(M_b) \sim 4.2 \text{ GeV}$, there is an additional $\frac{4}{3} \frac{\alpha_s}{\pi}$ factor which enters the cross section when switching from the on-shell to the $\overline{\text{MS}}$ scheme. This leads to an error of approximately 1% on the total cross section, over the M_H range that is relevant at the Tevatron. In contrast, according to very recent calculations [106–109], the $m_t \rightarrow \infty$ limit is a rather good approximation for the top-quark loop contribution to $\sigma(gg \rightarrow H)$ at NNLO as the higher order terms, when expanding the amplitude in power series of $M_H^2/(4m_t^2)$, lead to a difference that is smaller than one percent for $M_H \lesssim 300 \text{ GeV}$.

We turn now our attention to the electroweak radiative corrections and also estimate their associated error. As mentioned previously, while the $\mathcal{O}(\alpha)$ NLO corrections have been calculated with the exact dependence on the loop particle masses [32], the mixed QCD-electroweak corrections due to light quark loops at $\mathcal{O}(\alpha\alpha_s)$ have been evaluated [27] in the effective theory approach where the W, Z bosons have been integrated out and which is only valid for $M_H \ll M_W$. These contributions are approximately equal to the difference between the exact NLO electroweak corrections when evaluated in the complete factorisation and partial factorization schemes [27].

However, as the results for the mixed corrections are only valid at most for $M_H < M_W$ and given the fact that the companion δ_{EW} electroweak correction at $\mathcal{O}(\alpha)$ exhibits a completely different behavior below and above the $2M_W$ threshold,¹⁶ one should be cautious

¹⁵We thank Michael Spira for reminding us of this point.

¹⁶Indeed, the NLO electroweak correction δ_{EW} of ref. [32] is positive below the WW threshold $M_H \lesssim 2M_W$

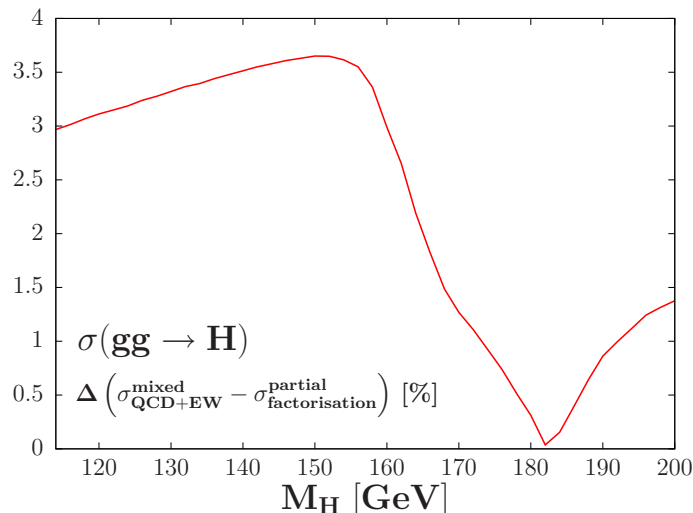


Figure 5. Relative difference (in %) between the complete factorisation and partial factorisation approaches for the electroweak radiative corrections to the NLO $gg \rightarrow H$ cross section at the Tevatron as a function of M_H .

and assign an uncertainty to this mixed QCD-electroweak correction. Conservatively, we have chosen to assign an error that is of the same size as the $\mathcal{O}(\alpha_s)$ contribution itself. This is equivalent to assigning an error to the full $\mathcal{O}(\alpha)$ contribution that amounts to the difference between the correction obtained in the complete factorisation and partial factorisation schemes as done in ref. [32]. As pointed out in the latter reference, this reduces to adopting the usual and well-established procedure that has been used at LEP for attributing uncertainties due to unknown higher order effects. Doing so, one obtains an uncertainty ranging from 1.5% to 3.5% for Higgs masses below $M_H \lesssim 2M_W$ and below 1.5% for larger Higgs masses as is shown in figure 5.

Finally, we should note that we do not address here the issue of the threshold effects from virtual W and Z bosons which lead to spurious spikes in the $\mathcal{O}(\alpha)$ electroweak correction in the mass range $M_H = 160\text{--}190$ GeV which includes the Higgs mass domain that is most relevant at the Tevatron (the same problem occurs in the case of the $p\bar{p} \rightarrow HV$ cross sections once the electroweak corrections are included). These singularities are smoothed by including the finite widths of the W/Z bosons, a procedure which might introduce potential additional theoretical ambiguities that we will ignore in the present analysis.

3.3 Uncertainties from the PDFs and α_s

Another major source of theoretical uncertainties on production cross sections and distributions at hadron colliders is due to the still imperfect parametrisation of the parton

for which the effective approach is valid in this case and turns to negative for $M_H \gtrsim 2M_Z$ for which the effective approach cannot be applied and the amplitude develops imaginary parts. This behavior can also be seen in figure 5 which, up to the overall normalisation, is to a very good approximation the δ_{EW} correction factor given in figure 1 of ref. [32] for $M_H \lesssim 2M_Z$.

distribution functions. Within a given parametrisation, for example the one in the MSTW scheme, these uncertainties are estimated as follows [47, 110], for an earlier discussion of the PDF uncertainties in the Higgs production cross sections at hadron colliders see for instance [111]. The scheme is based on a matrix method which enables a characterization of a parton parametrization in the neighborhood of the global χ^2 minimum fit and gives an access to the uncertainty estimation through a set of PDFs that describes this neighborhood. The corresponding PDFs are constructed by:

- (i) performing a global fit of the data using N_{PDF} free parameters ($N_{\text{PDF}} = 15$ or 20 , depending on the scheme); this provides the nominal PDF or reference set denoted by S_0 ;
- (ii) the global χ^2 of the fit is increased to a given value $\Delta\chi^2$ to obtain the error matrix;
- (iii) the error matrix is diagonalized to obtain N_{PDF} eigenvectors corresponding to N_{PDF} independent directions in the parameter space;
- (iv) for each eigenvector, up and down excursions are performed in the tolerance gap, $T = \sqrt{\Delta\chi_{\text{global}}^2}$, leading to $2N_{\text{PDF}}$ sets of new parameters, denoted by S_i , with $i = 1, 2N_{\text{PDF}}$.

These sets of PDFs can be used to calculate the uncertainty on a cross section σ in the following way: one first evaluates the cross section with the nominal PDF S_0 to obtain the central value σ_0 , and then calculates the cross section with the S_i PDFs, giving $2N_{\text{PDF}}$ values σ_i , and defines, for each σ_i value, the deviations

$$\sigma_i^\pm = |\sigma_i - \sigma_0| \quad \text{when } \sigma_i \gtrless \sigma_0 \tag{3.5}$$

The uncertainties are summed quadratically to calculate the cross section, including the error from the PDFs that are given at the 90% confidence level (CL),

$$\sigma_0 \Big|_{-\Delta\sigma_{\text{PDF}}^-}^{+\Delta\sigma_{\text{PDF}}^+} \quad \text{with } \Delta\sigma_{\text{PDF}}^\pm = \left(\sum_i \sigma_i^{\pm 2} \right)^{1/2} \tag{3.6}$$

The procedure outlined above has been applied to estimate the PDF uncertainties in the Higgs production cross sections in the gluon-gluon fusion mechanism at the Tevatron in refs. [25, 27]. This has led to a 90% CL uncertainty of $\approx 6\%$ for the low mass range $M_H \approx 120$ GeV to $\approx 10\%$ in the high mass range, $M_H \approx 200$ GeV. These uncertainties have been adopted in the CDF/D0 combined Higgs search and represent the second largest source of errors after the scale variation. We believe that, at least in the case of the gg fusion mechanism, restricting to the procedure described above largely underestimates the PDF uncertainties for at least the two reasons discussed below.

First of all, the MSTW collaboration [42, 43] is not the only one which uses the above scheme for PDF error estimates, as the CTEQ [61, 62] and ABKM [63, 64] collaborations, for instance, also provide similar schemes (besides the NNPDF set [112], an additional NNLO PDF set [113] has recently appeared and it also allows for error estimates). It is

thus more appropriate to compare the results given by the three different sets and take into account the possibly different errors that one obtains. In addition, as the parameterisations of the PDFs are different in the three schemes, one might obtain different central values for the cross sections and the impact of this difference should also be addressed.¹⁷

In our analysis, we will take into account these two aspects and investigate the PDF uncertainties given separately by the three MSTW, ABKM and CTEQ schemes, but we also compare the possibly different central values given by the three schemes. Note that despite of the fact that the CTEQ collaboration does not yet provide PDF sets at NNLO, one can still use the available NLO sets, evaluating the PDF errors on the NLO cross sections and take these errors as approximately valid at NNLO, once the cross sections are properly rescaled by including the NNLO corrections. For the sake of error estimates, this procedure should provide a good approximation.

In the case of the $gg \rightarrow H$ cross section at the Tevatron, the 90% CL PDF errors using the three schemes discussed above are shown in figure 6 as a function of M_H . The spread of the cross section due to the PDF errors is approximately the same in the MSTW and CTEQ schemes, leading to an uncertainty band of less than 10% in both cases. For instance, in the MSTW scheme and in agreement with refs. [25, 27], we obtain a $\sim \pm 6\%$ error for $M_H = 120$ GeV and $\sim \pm 9\%$ for $M_H = 180$ GeV; the errors are only slightly asymmetric and for $M_H = 160$ GeV, one has $\Delta\sigma_{\text{PDF}}^+/\sigma = +8.1\%$ and $\Delta\sigma_{\text{PDF}}^-/\sigma = -8.6\%$. The errors are relatively smaller in the ABKM case in the entire Higgs mass range and, for instance, one obtains a $\Delta\sigma_{\text{PDF}}^\pm/\sigma \approx \pm 5\%$ (7%) error for $M_H = 120$ (180) GeV.

A more important issue is the very large discrepancy between the central values of the cross sections calculated with the MSTW and CTEQ PDFs on the one hand and the ABKM set of PDFs, on the other hand.¹⁸ Indeed, the use of the ABKM parametrisation results in a cross section that is $\sim 25\%$ smaller than the cross section evaluated with the MSTW or CTEQ PDFs. Thus, even if the PDF uncertainties evaluated within a given scheme turn out to be relatively small and apparently well under control, the spread of the cross sections due to the different parameterisations can be much more important.

If one uses the old way of estimating the PDF uncertainties (i.e. before the advent of the PDF error estimates within a given scheme) by comparing the results given by different PDF parameterisations, one arrives at an uncertainty defined as

$$\begin{aligned} \Delta\sigma_{\text{PDF}}^+ &= \max(\sigma_{\text{MSTW}}^0, \sigma_{\text{CTEQ}}^0, \sigma_{\text{ABKM}}^0) - \sigma_{\text{MSTW}}^0 \\ \Delta\sigma_{\text{PDF}}^- &= \sigma_{\text{MSTW}}^0 - \min(\sigma_{\text{MSTW}}^0, \sigma_{\text{CTEQ}}^0, \sigma_{\text{ABKM}}^0) \end{aligned} \tag{3.7}$$

where the central value of the $gg \rightarrow H$ cross section is taken to be that given by the MSTW nominal set S_0 (we refrain here from adding the uncertainties obtained within the same PDF set, which would increase the error by another 5% to 7%). Hence, for $M_H = 160$

¹⁷This difference should not come as a surprise as, even within the same scheme, there are large differences when the PDF sets are updated. For instance, as also pointed out in refs. [25, 27], $\sigma^{\text{NNLO}}(gg \rightarrow H)$ evaluated with the MSTW2004 set is different by more than 10% compared to the current value obtained with the MSTW2008 set, as a result of a corrected treatment of the b, c densities among other improvements.

¹⁸Besides refs. [63, 64, 110], this problem has also been briefly mentioned in the discussion of ref. [114] which appeared during the final stage of our work.

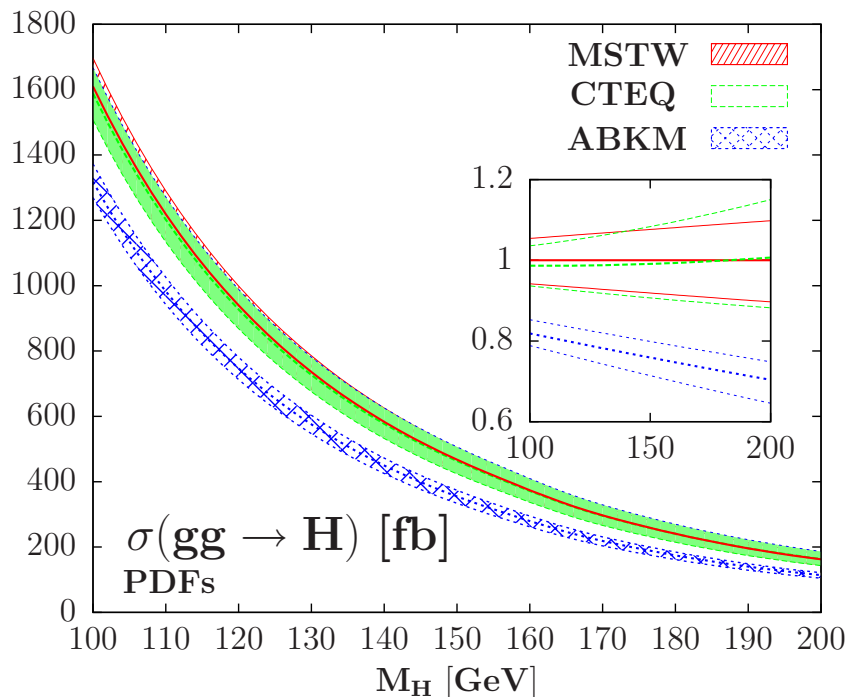


Figure 6. The central values and the 90% CL PDF uncertainty bands in the NNLO cross section $\sigma(gg \rightarrow H + X)$ at the Tevatron when evaluated within the MSTW, CTEQ and ABKM schemes. In the insert, shown in percentage are the deviations within a given scheme and the CTEQ and ABKM central values when the cross sections are normalized to the MSTW central value.

GeV for instance, one would have $\Delta\sigma_{\text{PDF}}^+ \approx 1\%$ given by the small difference between the CTEQ and MSTW central values of the cross section and $\Delta\sigma_{\text{PDF}}^- \approx -25\%$ given by the large difference between the ABKM and MSTW central values.

However, we would like to keep considering the MSTW scheme at least for the fact that it includes the di-jet Tevatron data which are crucial in this context. But we would also like to understand the very large difference in the $gg \rightarrow H$ cross section when evaluated with the MSTW/CTEQ and ABKM sets. This difference results not only from the different gluon densities used (and it is well known that these densities are less severely constrained by experimental data than light quark densities), but is also due to the different values of the strong coupling constant which is fitted altogether with the PDF sets. Indeed, the value of α_s and its associated error play a crucial role in the presently discussed production process. For instance, the α_s value used in the ABKM set, $\alpha_s(M_Z^2) = 0.1129 \pm 0.0014$ at NLO in the BMSM scheme [115], is $\approx 3\sigma$ smaller than the one in the MSTW set (see below). Note also that within the dynamical set of PDFs recently proposed in Ref [113], one obtains too an NLO α_s value that is smaller than the MSTW value but with a slightly larger uncertainty, $\alpha_s(M_Z^2) = 0.1124 \pm 0.0020$.

As the $gg \rightarrow H$ mechanism is mediated by triangular loops involving the heavy top and bottom quarks, the cross section $\sigma(gg \rightarrow H)$ is at $\mathcal{O}(\alpha_s^2)$ already in the Born approximation and the large NLO and NNLO QCD contributions are, respectively, of $\mathcal{O}(\alpha_s^3)$

and $\mathcal{O}(\alpha_s^4)$. Since the corresponding K -factors are very large at the Tevatron, $K_{\text{NLO}} \sim 2$ and $K_{\text{NNLO}} \sim 3$, a one percent uncertainty in the input value of α_s will generate a $\approx 3\%$ uncertainty in $\sigma^{\text{NNLO}}(gg \rightarrow H)$. If, for instance, one uses the value of α_s at NLO and its associated experimental uncertainty that is fitted in the global analysis of the hard scattering data performed by the MSTW collaboration [110]

$$\alpha_s(M_Z^2) = 0.1202 \begin{matrix} +0.0012 \\ -0.0015 \end{matrix} \text{ (68\%CL)} \quad \begin{matrix} +0.0032 \\ -0.0039 \end{matrix} \text{ (90\%CL)} \quad \text{at NLO} \quad (3.8)$$

leading to $\alpha_s(M_Z^2) = 0.1171 \begin{matrix} +0.0014 \\ -0.0014 \end{matrix}$ (68%CL) at NNLO, by naively plaguing the 90% CL errors on α_s in the perturbative series of the partonic cross section but using the best-fit PDF set, one arrives at an uncertainty on the $gg \rightarrow H$ cross section that is of the order of $\Delta\sigma/\sigma \approx \pm 8\%$ at the Tevatron, over the entire $115 \text{ GeV} \lesssim M_H \lesssim 200 \text{ GeV}$ range.

Nevertheless, such a naive procedure cannot be applied in practice as, in general, α_s is fitted together with the PDFs: the PDF sets are only defined for the special value of α_s obtained with the best fit and, to be consistent, this best value of α_s that we denote α_s^0 , should also be used for the partonic part of the cross section. This adds to the fact that there is an interplay between the PDFs and the value of α_s and, for instance, a larger value of α_s would lead to a smaller gluon density at low x [110].

Fortunately enough, the MSTW collaboration released very recently a new set-up which allows for a simultaneous evaluation of the errors due to the PDFs and those due to the experimental uncertainties on α_s of eq. (3.8), taking into account the possible correlations [110]. The procedure to obtain the different PDFs and their associated errors is similar to the one discussed before, but provided is a collection of five PDF+error sets for different α_s values: the best fit value α_s^0 and its 68% CL and 90% CL maximal and minimal values. Using the following equations to calculate the PDF error for a fixed value of α_s ,

$$\begin{aligned} (\Delta\sigma_{\text{PDF}}^{\alpha_s})_+ &= \sqrt{\sum_i \left\{ \max \left[\sigma(\alpha_s, S_i^+) - \sigma(\alpha_s^0, S_0), \sigma(\alpha_s, S_i^-) - \sigma(\alpha_s^0, S_0), 0 \right] \right\}^2}, \\ (\Delta\sigma_{\text{PDF}}^{\alpha_s})_- &= \sqrt{\sum_i \left\{ \max \left[\sigma(\alpha_s^0, S_0) - \sigma(\alpha_s, S_i^+), \sigma(\alpha_s^0, S_0) - \sigma(\alpha_s, S_i^-), 0 \right] \right\}^2}, \end{aligned} \quad (3.9)$$

one then compares these five different values and finally arrives, with α_s^0 as the best-fit value of α_s given by the central values of eq. (3.8) and S_0 the nominal PDF set with this α_s value, at the 90% CL PDF+ $\Delta^{\text{exp}}\alpha_s$ errors given by [110]

$$\begin{aligned} \Delta\sigma_{\text{PDF}+\alpha_s^{\text{exp}}}^+ &= \max_{\alpha_s} \left(\left\{ \sigma(\alpha_s^0, S_0) + (\Delta\sigma_{\text{PDF}}^{\alpha_s})_+ \right\} \right) - \sigma(\alpha_s^0, S_0), \\ \Delta\sigma_{\text{PDF}+\alpha_s^{\text{exp}}}^- &= \sigma(\alpha_s^0, S_0) - \min_{\alpha_s} \left(\left\{ \sigma(\alpha_s^0, S_0) - (\Delta\sigma_{\text{PDF}}^{\alpha_s})_- \right\} \right). \end{aligned} \quad (3.10)$$

Using this procedure, we have evaluated the PDF+ $\Delta^{\text{exp}}\alpha_s$ uncertainty on the NNLO $gg \rightarrow H$ total cross section at the Tevatron and the result is displayed in the left-hand side of figure 7 as a function of M_H . The PDF+ $\Delta^{\text{exp}}\alpha_s$ error ranges from $\approx \pm 11\%$ for $M_H = 120 \text{ GeV}$ to $\approx \pm 14\%$ for $M_H = 180 \text{ GeV}$ with, again, a slight asymmetry between the upper and lower values; for a Higgs mass $M_H = 160 \text{ GeV}$, one has $\Delta\sigma_{\text{PDF}+\alpha_s}^{\pm}/\sigma = \begin{matrix} +12.8\% \\ -12.0\% \end{matrix}$.

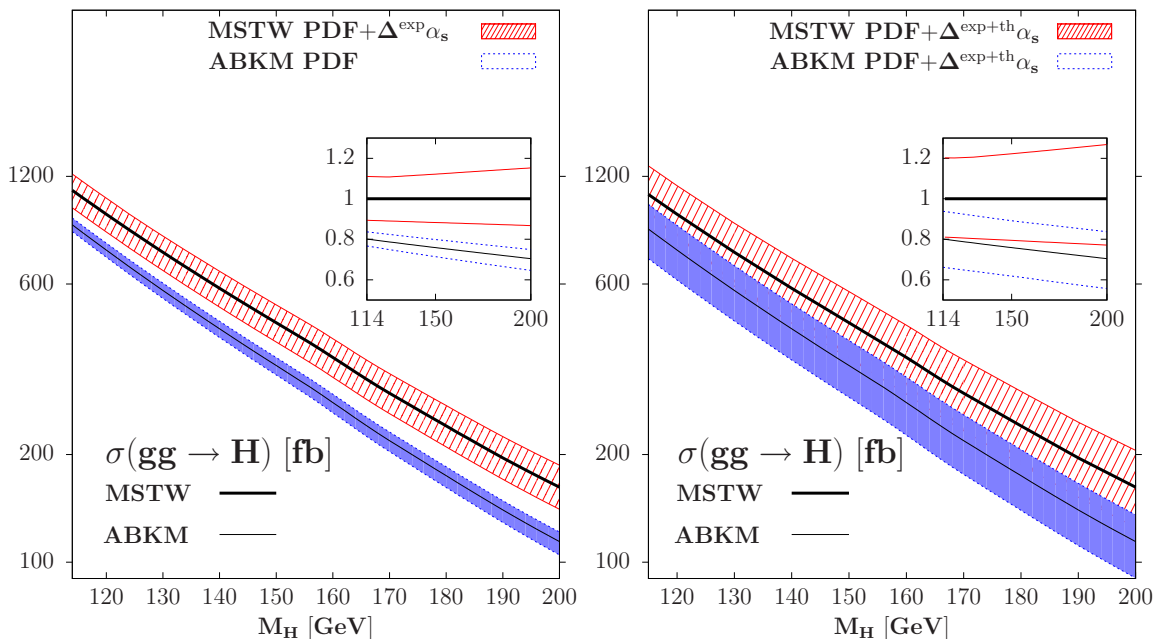


Figure 7. Left: the PDF+ $\Delta^{\text{exp}}\alpha_s$ uncertainties in the MSTW scheme and the PDF uncertainties in the ABKM schemes on the $gg \rightarrow H$ cross section at the Tevatron as a function of M_H . Right: the PDF+ $\Delta^{\text{exp}}\alpha_s + \Delta^{\text{th}}\alpha_s$ uncertainties in the MSTW scheme using the new set-up and the PDF+ $\Delta^{\text{exp}}\alpha_s + \Delta^{\text{th}}\alpha_s$ error in the ABKM scheme using our naive procedure. In the inserts, shown are the same but with the cross sections normalized to the MSTW central cross section.

That is, the experimental uncertainty on α_s adds a $\approx 5\%$ error to the PDF error alone over the entire M_H range relevant at the Tevatron. This is a factor of ≈ 1.5 less than the naive guess made previously, as a result of the correlation between the PDFs and the α_s value.

Nevertheless, this larger PDF+ $\Delta^{\text{exp}}\alpha_s$ uncertainty compared to the PDF uncertainty alone does not yet reconcile the evaluation of MSTW and ABKM (in this last scheme the $\Delta^{\text{exp}}\alpha_s$ uncertainty has not been included since no PDF set with an error on α_s is provided) of the $gg \rightarrow H$ cross section at the Tevatron, the difference between the lowest MSTW value and the highest ABKM value being still at the level of $\approx 10\%$.

So far, only the impact of the experimental errors on α_s has been discussed, while it is well known that the strong coupling constant is also plagued by theoretical uncertainties due to scale variation, ambiguities in heavy quark flavor scheme definition, etc.. In ref. [42, 43] this theoretical error has been estimated to be at least $\Delta^{\text{th}}\alpha_s = \pm 0.003$ at NLO (± 0.002 at NNLO) while the estimate of ref. [116] leads to a slightly larger uncertainty, $\Delta^{\text{th}}\alpha_s = \pm 0.0033$. Unfortunately, this theoretical error is not taken into account in the MSTW PDF+ $\Delta\alpha_s$ error set-up discussed above, nor is addressed by any of the other PDF schemes.

Adopting the smallest of the 1σ α_s errors at NLO quoted above, i.e.

$$\Delta^{\text{th}}\alpha_s = 0.003, \tag{3.11}$$

we have evaluated the uncertainty due this theoretical error on $\sigma^{\text{NNLO}}(gg \rightarrow H + X)$ at the Tevatron, following our naive and admittedly not entirely consistent first estimate of

the impact of the experimental error of α_s on the same cross section, i.e. using the values $\alpha_s^0 \pm 0.002$ in the partonic cross sections but the best-fit value α_s^0 in the best-fit PDF set. We obtain an error of $\approx 8\%$ on $\sigma^{\text{NNLO}}(gg \rightarrow H)$ for the M_H values relevant at the Tevatron.

There is nevertheless a more consistent way to address this issue of the theoretical uncertainty on α_s , thanks to a fixed- α_s NNLO PDF grid also provided by the MSTW collaboration, which is a set of central PDFs but at fixed values of α_s different from the best-fit value. Values of α_s in a range comprised between 0.107 and 0.127 in steps of 0.001 are selected, and thus include the values $\alpha_s^0 \pm 0.002$ that are interesting for our purpose. Using this PDF grid with the theoretical error on α_s of eq. (3.11) implemented, the upper and lower values of the cross sections will be given by

$$\begin{aligned} \Delta\sigma_{\text{PDF}+\alpha_s^{\text{th}}}^+ &= \sigma(\alpha_s^0 + \Delta^{\text{th}}\alpha_s, S_0(\alpha_s^0 + \Delta^{\text{th}}\alpha_s)) - \sigma(\alpha_s^0, S_0(\alpha_s^0)) \\ \Delta\sigma_{\text{PDF}+\alpha_s^{\text{th}}}^- &= \sigma(\alpha_s^0, S_0(\alpha_s^0)) - \sigma(\alpha_s^0 - \Delta^{\text{th}}\alpha_s, S_0(\alpha_s^0 - \Delta^{\text{th}}\alpha_s)) \end{aligned} \quad (3.12)$$

with again $S_0(\alpha_s)$ being the MSTW best-fit PDF set at the fixed α_s value which is either α_s^0 or $\alpha_s^0 \pm \Delta^{\text{th}}\alpha_s$. With this fixed- α_s PDF grid, we obtain an error of $\approx +10\%$ and $\approx -9\%$ on the total $gg \rightarrow H$ cross section at NNLO when one restricts to the range of Higgs masses relevant at the Tevatron, with a $\approx 1\%$ increase from $M_H = 115$ GeV to $M_H = 200$ GeV. This error is again very close to the naive estimate performed previously by considering only the impact of $\Delta^{\text{th}}\alpha_s$ on the partonic cross section. Note that despite of the fact that the uncertainty on α_s is a theoretical one and is not at the 90% CL, we will take the PDF+ $\Delta^{\text{th}}\alpha_s$ error that one obtains using the equations above to be at the 90% CL.

In the MSTW scheme, to obtain the total PDF+ α_s uncertainty, one then adds in quadrature the PDF+ $\Delta^{\text{exp}}\alpha_s$ and PDF+ $\Delta^{\text{th}}\alpha_s$ uncertainties,

$$\Delta\sigma_{\text{PDF}+\alpha_s^{\text{exp}}+\alpha_s^{\text{th}}}^\pm = \left((\Delta\sigma_{\text{PDF}+\alpha_s^{\text{exp}}}^\pm)^2 + (\Delta\sigma_{\text{PDF}+\alpha_s^{\text{th}}}^\pm)^2 \right)^{1/2}. \quad (3.13)$$

The result for the total PDF+ α_s 90% CL uncertainty on $\sigma^{\text{NNLO}}(gg \rightarrow H)$ in the MSTW scheme using the procedure outlined above is shown in the right-hand side of figure 7 as a function of M_H . It is compared to the result when the PDF error in the ABKM scheme is combined with the $\Delta^{\text{exp}}\alpha_s$ and $\Delta^{\text{th}}\alpha_s$ uncertainties using the naive procedure discussed previously as, in this case, no PDF with an α_s value different from that obtained with the best-fit is provided. One can see that the results given by the two parameterizations appear now to be consistent with each other as the two uncertainty bands overlap.

The net result of this exercise is that the total error on the $gg \rightarrow H$ cross section due to the PDF and the theoretical plus experimental uncertainties on α_s , is now rather significant and, in the case of the MSTW scheme to which we stick, it amounts to approximately ± 15 to 20% in the Higgs mass range relevant at the Tevatron. The uncertainty is, for instance, -15% and $+16.5\%$ for $M_H = 160$ GeV and is substantially smaller (for the minimal value of the cross section) than the error that would have been obtained using the old-fashioned estimate of the PDF errors by comparing different PDF sets, in which case one would have had an uncertainty of -26% and $+1\%$ compared to the MSTW central value.

The final error of $\approx \pm 15$ -20% is to be compared to the ± 6 -10% error obtained from the PDF uncertainty alone ($\approx \pm 8\%$ for $M_H = 160$ GeV), an amount which has been taken to

be the total PDF uncertainty in the CDF/D0 analysis of the Higgs signal. Thus, similarly to the scale variation, the PDF uncertainties, when the errors on α_s are taken into account, have been underestimated by at least a factor of two by the experiments.

4 Theoretical uncertainties in Higgs-strahlung

We now turn to the discussion of the theoretical uncertainties in the Higgs strahlung mechanism $q\bar{q} \rightarrow VH$, following the same line of arguments as in the previous section. Since in this case, the NNLO QCD corrections and the one-loop electroweak corrections have been obtained exactly and no effective approach was used, only the scale variation and the PDF+ α_s uncertainties have to be discussed. In addition, since the NNLO gluon-gluon fusion contribution to the cross section in the $p\bar{p} \rightarrow ZH$ case, which is absent in $p\bar{p} \rightarrow WH$, is very small at the Tevatron and because the scales and phase space are only slightly different for the $p\bar{p} \rightarrow WH$ and ZH processes, as the difference $(M_Z^2 - M_W^2)/\hat{s}$ is tiny, the kinematics and the K -factors for these two processes are very similar. We thus restrict our analysis to the WH channel but the same results hold for the ZH channel.

To evaluate the uncertainties due to the variation of the renormalisation and factorisation scales in the Higgs-strahlung processes, the choice of the variation domain is in a sense simpler than for the $gg \rightarrow H$ mechanism. Indeed, as the process at leading order is mediated solely by massive gauge boson exchange and, thus, does not involve strong interactions at the partonic level, only the factorisation scale μ_F appears when the partonic cross section is folded with the q and \bar{q} luminosities and there is no dependence on the renormalisation scale μ_R at this order. It is only at NLO, when gluons are exchanged between or radiated from the q, \bar{q} initial states, that both scales μ_R and μ_F appear explicitly.

Using our proposed criterion for the estimate of the perturbative higher order effects, we thus choose again to consider the variation domain of the scales from their central values, $\mu_0/\kappa \leq \mu_R, \mu_F \leq \kappa\mu_0$ with $\mu_0 = M_{\text{HW}}$, of the NLO cross section instead of that of the LO cross section to determine the value of the factor κ to be used at NNLO. We display in the left-hand side of figure 8 the variation of the NLO cross section $\sigma^{\text{NLO}}(p\bar{p} \rightarrow WH)$ at the Tevatron as a function of M_H for three values of the constant κ which defines the range spanned by the scales, $M_{\text{HW}}/\kappa \leq \mu_R, \mu_F \leq \kappa M_{\text{HW}}$. One sees that, in this case, a value $\kappa = 2$ is sufficient (if the scales μ_R and μ_F are varied independently in the chosen domain) in order that the uncertainty band at NLO reaches the central value of the cross section at NNLO. In fact, the NLO uncertainty band would have been only marginally affected if one had chosen the values $\kappa = 3, 4$ or even 5. This demonstrates that the cross sections for the Higgs-strahlung processes, in contrast to $gg \rightarrow H$, are very stable against scale variation, a result that is presumably due to the smaller $q\bar{q}$ color charges compared to gluons, $\approx C_F/C_A$, that lead to more moderate QCD corrections.

In the right-hand side of figure 8, the NNLO $p\bar{p} \rightarrow WH$ total cross section is displayed as a function of M_H for a scale variation $\frac{1}{2}M_{\text{HW}} \leq \mu_R, \mu_F \leq 2M_{\text{HW}}$. Contrary to the $gg \rightarrow H$ mechanism, the scale variation within the chosen range is rather mild and only a $\sim 0.7\%$ (at low M_H) to 1.2% (at high M_H) uncertainty is observed for the relevant Higgs mass range at the Tevatron. This had to be expected as the K -factors in the Higgs-

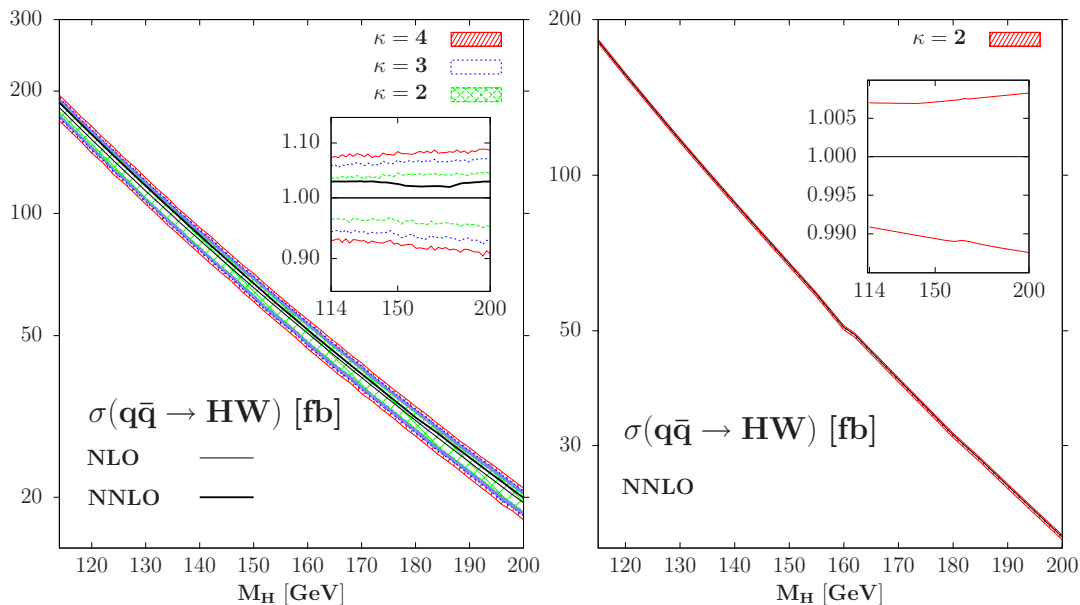


Figure 8. Left: the scale dependence of $\sigma(p\bar{p} \rightarrow WH)$ at NLO for variations $M_{\text{HV}}/\kappa \leq \mu_R, \mu_F \leq \kappa M_{\text{HV}}$ with $\kappa = 2, 3$ and 4, compared to the NNLO value; in the insert, shown are the variations in percentage and where the NNLO cross section is normalized to the NLO one. Right: the scale dependence of $\sigma(p\bar{p} \rightarrow WH)$ at NNLO for a variation in the domains $M_{\text{HV}}/2 \leq \mu_R = \mu_F \leq 2M_{\text{HV}}$; the relative deviations from the central value are shown in the insert.

strahlung processes, $K_{\text{NLO}} \approx 1.4$ and $K_{\text{NNLO}} \approx 1.5$, are substantially smaller than those affecting the gg fusion mechanism and one expects perturbation theory to have a better behavior in the former case. This provides more confidence that the Higgs-strahlung cross section is stable against scale variation and, thus, that higher order effects should be small.

For the estimate of the uncertainties due to the PDFs in associated Higgs production with a W boson, $p\bar{p} \rightarrow WH$ (again, the output is similar for $p\bar{p} \rightarrow ZH$ except from the overall normalisation, despite of the different initial state (anti)quarks), the same exercise made in section 3.3 for the gg fusion mechanism has been repeated. The results are shown in figures 9 and 10 for Tevatron energies as a function of M_H . Figure 9 displays the spread of the $p\bar{p} \rightarrow WH$ cross section due to the PDF uncertainties alone in the MSTW, CTEQ and ABKM schemes and, again in this case, the uncertainty bands are similar in the CTEQ and MSTW schemes and lead to an error of about 4%; the band is, however, slightly larger in the ABKM scheme. Here also appears a discrepancy between the MSTW/CTEQ and the ABKM central values, the cross section with the PDFs from ABKM being this time about 10% larger than that obtained with the other sets. However, in contrast to the $gg \rightarrow H$ case, the MSTW/CTEQ and ABKM uncertainty bands almost touch each other.

In the left-hand side of figure 10, we show the bands resulting from the PDF+ $\Delta^{\text{exp}}\alpha_s$ uncertainty in the MSTW mixed scheme, while the right-hand side of the figure shows the uncertainty bands when the additional theoretical error $\Delta^{\text{th}}\alpha_s$ is included in both the MSTW scheme using eq. (3.13) and ABKM scheme using the naive estimate of eq. (3.12).

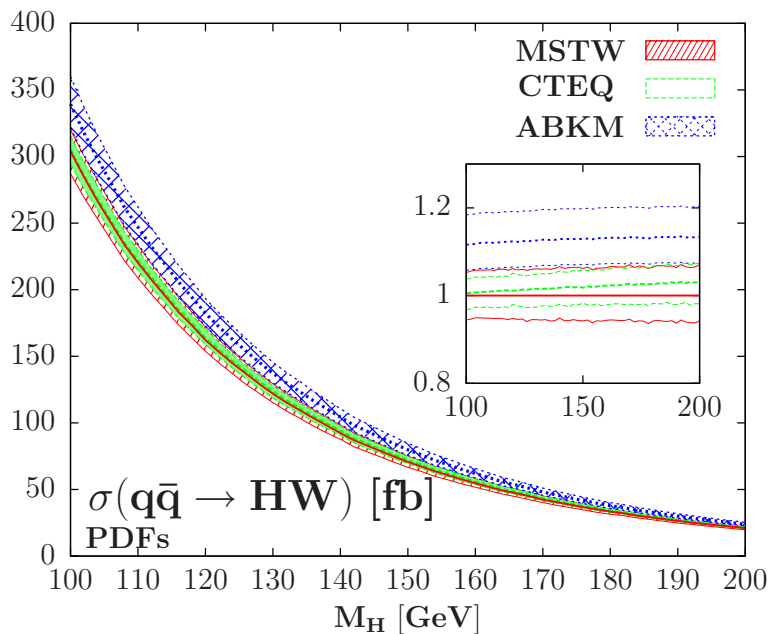


Figure 9. The central values and the PDF uncertainties in the cross section $\sigma(p\bar{p} \rightarrow WH)$ at the Tevatron when evaluated within the MSTW, CTEQ and ABKM schemes. In the insert, the relative deviations from the central MSTW value are shown.

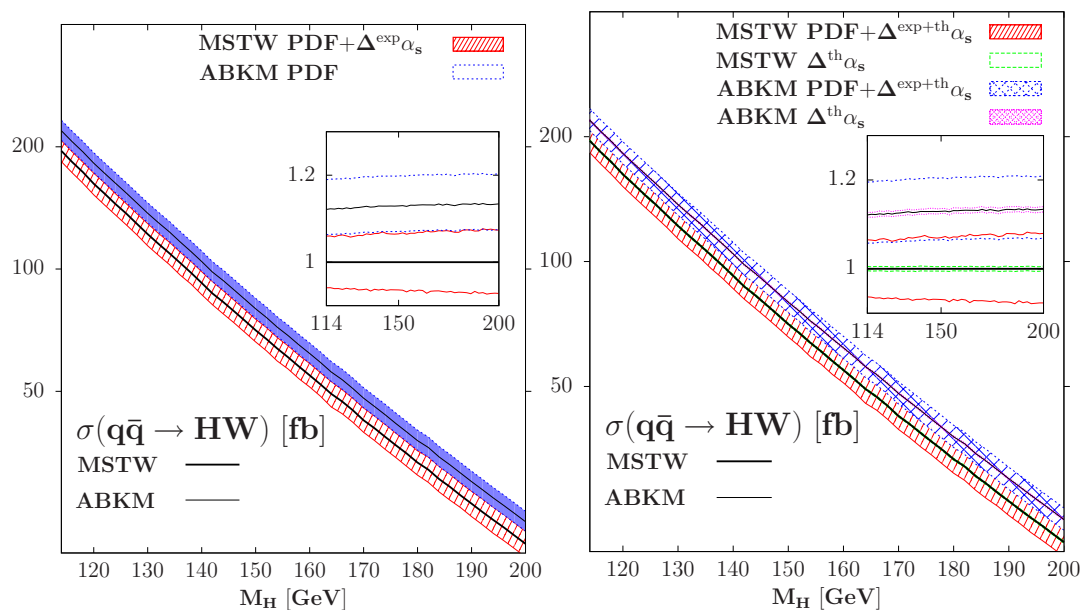


Figure 10. Left: the PDF uncertainties in the MSTW and ABKM schemes when the additional experimental errors on α_s is included in MSTW as discussed in the text; in the insert, the relative deviations from the central MSTW value are shown. Right: the same as in a) but when the theoretical error on α_s is added in both the MSTW and ABKM cases.

As expected, the errors due to the imprecise value of α_s are much smaller than in the $gg \rightarrow H$ mechanism, as in Higgs-strahlung, the process does not involve α_s in the Born approximation and the K -factors are reasonably small, $K_{\text{NNLO}} \lesssim 1.5$. Hence, $\Delta^{\text{exp}}\alpha_s$ generates an additional error that is about $\approx 2\%$ when included in the PDF fits, while the error due to $\Delta^{\text{th}}\alpha_s$ is about one to two percent.

Nevertheless, the total PDF+ $\Delta^{\text{exp}}\alpha_s$ + $\Delta^{\text{th}}\alpha_s$ uncertainty is at the level of $\approx 7\text{--}8\%$ in the MSTW scheme, i.e. slightly larger than the errors due to the PDFs alone, and arranges again so that the MSTW and ABKM uncertainty bands have a significant overlap.

5 The total uncertainties at the Tevatron

The analysis of the Higgs production cross section in the $gg \rightarrow H$ process at the Tevatron, as well as the various associated theoretical uncertainties, is summarized in table 2. For a set of Higgs mass values that is relevant at the Tevatron (we choose a step of 5 GeV as done by the CDF and D0 experiments [8] except in the critical range 160–170 GeV where a 2 GeV step is adopted), the second column of the table gives the central values of the total cross section at NNLO (in fb) for the renormalisation and factorisation scale choice $\mu_R = \mu_F = M_H$, when the partonic cross sections are folded with the MSTW parton densities. The following columns give the errors on the central value of the cross section originating from the various sources discussed in section 3, namely, the uncertainties due to the scale variation in the adopted range $\frac{1}{3}M_H \leq \mu_R, \mu_F \leq 3M_H$, the 90% CL errors due to the MSTW PDF, PDF+ $\Delta^{\text{exp}}\alpha_s$ and PDF+ $\Delta^{\text{exp}}\alpha_s$ + $\Delta^{\text{th}}\alpha_s$ uncertainties as well as the estimated uncertainties from the use of the effective approach in the calculation of the NNLO QCD (the b -quark loop contribution and its interference with the top-quark loop) and electroweak (difference between the complete and partial factorisation approaches) radiative corrections.

The largest of these errors, $\sim 20\%$, is due to the scale variation, followed by the PDF+ $\Delta^{\text{exp}}\alpha_s$ + $\Delta^{\text{th}}\alpha_s$ uncertainties which are at the level of $\approx 15\%$; the errors due to the effective theory approach (including that due to the definition of the b -quark mass) are much smaller, being of the order of a few percent for both the QCD and electroweak parts.

The next important issue is how to combine these various uncertainties. In accord with ref. [26], we do not find any obvious justification to add these errors in quadrature as done, for instance, by the CDF and D0 collaborations¹⁹ [117–119]. Indeed, while the PDF+ α_s uncertainty might have some statistical ground, the scale uncertainty as well as the uncertainties due to the use of the effective approach are purely theoretical errors. On the other hand, one cannot simply add these errors linearly as is generally done for theoretical errors, the reason being a possibly strong interplay between the scale chosen for the process, the value of α_s (which evolves with the scales) and thus the PDFs (since the gluon density, for instance, is sensitive to the exact value of α_s as mentioned previously). Here, we propose a simple procedure to combine at least the two largest uncertainties,

¹⁹In earlier analyses, the CDF collaboration [117, 119] adds in quadrature the 10.9% scale uncertainty obtained at NNLL with a scale variation in the range $\frac{1}{2}M_H \leq \mu_R, \mu_F \leq 2M_H$ with a 5.1% uncertainty due to the errors on the MSTW PDFs (not including the errors from α_s), resulting in a 12% total uncertainty. The D0 collaboration [118, 119] assigns an even smaller total error, 10%, to the production cross section.

those due to the scale variation and to the PDF+ α_s uncertainties, that is in our opinion more adequate and avoids the drawbacks of the two other possibilities mentioned above.

The procedure that we propose is as follows. One first derives the maximal and minimal values of the production cross sections when the renormalisation and factorisation scales are varied in the adopted domain, that is, $\sigma_0 \pm \Delta\sigma_\mu^\pm$ with σ_0 being the cross section evaluated for the central scales $\mu_R = \mu_F = \mu_0$ and the deviations $\Delta\sigma_\mu^\pm$ given in eq. (3.2). One then evaluates on these maximal and minimal cross sections from scale variation, the PDF+ $\Delta^{\text{exp}}\alpha_s$ as well as the PDF+ $\Delta^{\text{th}}\alpha_s$ uncertainties (combined in quadrature) using the new MSTW set-up, i.e as in eq. (3.13) but with σ_0 replaced by $\sigma_0 \pm \Delta\sigma_\mu^\pm$.

One then obtains the maximal and minimal values of the cross section when scale, PDF and α_s (both experimental and theoretical) uncertainties are included,

$$\begin{aligned}\sigma_{\text{max}}^{\mu+\text{PDF}+\alpha_s} &= (\sigma_0 + \Delta\sigma_\mu^+) + \Delta(\sigma_0 + \Delta\sigma_\mu^+)_{\text{PDF}+\alpha_s^{\text{exp}}+\alpha_s^{\text{th}}}, \\ \sigma_{\text{min}}^{\mu+\text{PDF}+\alpha_s} &= (\sigma_0 - \Delta\sigma_\mu^-) - \Delta(\sigma_0 - \Delta\sigma_\mu^-)_{\text{PDF}+\alpha_s^{\text{exp}}+\alpha_s^{\text{th}}}.\end{aligned}\tag{5.1}$$

To these new maximal and minimal cross sections, one should then add the much smaller errors originating from the other sources such as, in the case of the $gg \rightarrow H$ process, those due to the missing b -quark loop and the mixed QCD-electroweak corrections at NNLO. This last addition can be done linearly as the errors from the use of the effective theory approach are purely theoretical ones and do not depend on the scale choice in practice.²⁰

The two last columns of table 2 display the maximal and minimal deviations of the $gg \rightarrow H$ cross section at the Tevatron when all errors are added, as well as the percentage deviations of the cross section from the central value. We should note that the actual PDF+ α_s error and the error from the use of the effective theory approach are different from those of table 2, which are given for the best value of the cross section, obtained for the central scale choice $\mu_F = \mu_R = M_H$; nevertheless, the relative or percentage errors are approximately the same for σ_0 and $\sigma_0 \pm \Delta\sigma_\mu^\pm$.

One observes from table 2 that when all theoretical errors are combined, there is a large variation of the $gg \rightarrow H$ cross section. The percentage total error on the cross section is approximately the same in the entire Higgs mass range that is indicated and is significant, the lower and upper values being $\approx 40\%$ smaller or $\approx 50\%$ larger than the central value. For $M_H = 160$ GeV for instance, one obtains a spread from the central value $\sigma_0 = 374$ fb which amounts to $\sigma_{\text{max}} = 552$ fb and $\sigma_{\text{min}} = 225$ fb, a spread that leads to a percentage error of $\Delta\sigma_0/\sigma_0 = -39.7\%$ and $+47.6\%$.

This is again summarized in figure 11, where the total uncertainty band obtained in our analysis is confronted to the uncertainty band that one obtains when adding in quadrature the scale uncertainty for $\frac{1}{2}M_H \leq \mu_R, \mu_F \leq 2M_H$ and the PDF error only (without the errors on α_s) as assumed in the CDF/D0 analysis. Furthermore, in the latter case, we use the resummed NNLL cross sections given in ref. [25] which is $\sim 15\%$ higher than the cross

²⁰In the case of the b -loop contribution, the K -factor when varying the scale from the central value M_H to the values $\approx \frac{1}{3}M_H$ or $\approx 3M_H$ which maximise and minimise the cross section, might be slightly different and thus, the error will not be exactly that given in table 2. However, since the entire effect is very small, we will ignore this tiny complication here.

M_H	$\sigma_{gg \rightarrow H}^{\text{NNLO}}$ [fb]	scale	PDF	PDF + α_s^{exp}	α_s^{th}	EW	b-loop	total	% total
115	1068	+244 -226	+65 -69	+118 -113	+97 -90	+32 -32	+28 -28	+507 -416	+47% -39%
120	940	+212 -199	+59 -63	+103 -101	+87 -79	+29 -29	+25 -25	+446 -368	+47% -39%
125	830	+185 -176	+54 -58	+90 -90	+78 -71	+27 -27	+21 -21	+394 -327	+47% -39%
130	736	+163 -156	+50 -53	+82 -81	+70 -63	+24 -24	+18 -18	+349 -291	+47% -40%
135	654	+144 -139	+46 -49	+74 -73	+63 -56	+22 -22	+16 -16	+312 -260	+48% -40%
140	584	+128 -124	+42 -45	+68 -66	+57 -51	+21 -21	+14 -14	+279 -234	+48% -40%
145	522	+113 -111	+39 -41	+62 -60	+52 -46	+19 -19	+12 -12	+250 -209	+48% -40%
150	468	+101 -99	+36 -38	+57 -55	+47 -41	+17 -17	+11 -11	+225 -188	+48% -40%
155	419	+90 -89	+33 -35	+52 -50	+43 -37	+15 -15	+9 -9	+202 -169	+48% -40%
160	374	+79 -80	+30 -32	+48 -45	+39 -34	+11 -11	+8 -8	+178 -149	+48% -40%
162	357	+76 -76	+29 -31	+46 -43	+37 -32	+9 -9	+7 -7	+169 -141	+47% -39%
164	340	+72 -72	+28 -30	+44 -41	+36 -31	+7 -7	+7 -7	+159 -133	+47% -39%
165	333	+70 -71	+28 -29	+44 -41	+35 -30	+7 -7	+7 -7	+156 -130	+47% -39%
166	324	+69 -69	+27 -29	+43 -40	+34 -29	+6 -6	+7 -7	+151 -126	+47% -39%
168	310	+65 -66	+26 -28	+41 -38	+33 -28	+5 -5	+7 -7	+143 -119	+46% -38%
170	297	+63 -63	+25 -27	+40 -37	+32 -27	+4 -4	+6 -6	+137 -114	+46% -38%
175	267	+56 -57	+23 -25	+37 -33	+29 -25	+3 -3	+5 -5	+123 -102	+46% -38%
180	240	+50 -51	+22 -23	+34 -31	+26 -22	+1 -1	+5 -5	+109 -90	+45% -38%
185	217	+45 -46	+20 -21	+31 -28	+24 -20	+1 -1	+5 -5	+99 -82	+46% -38%
190	196	+41 -42	+18 -19	+28 -25	+22 -18	+2 -2	+4 -4	+91 -75	+46% -38%
195	178	+37 -38	+17 -18	+26 -23	+20 -17	+2 -2	+3 -3	+83 -69	+47% -39%
200	162	+33 -35	+16 -17	+25 -22	+19 -15	+2 -2	+3 -3	+77 -63	+47% -39%

Table 2. The NNLO total Higgs production cross sections in the $gg \rightarrow H$ process at the Tevatron (in fb) for given Higgs mass values (in GeV) with the corresponding uncertainties from the various sources discussed in section 3, as well as the total uncertainty when all errors are added using the procedure described in the text.

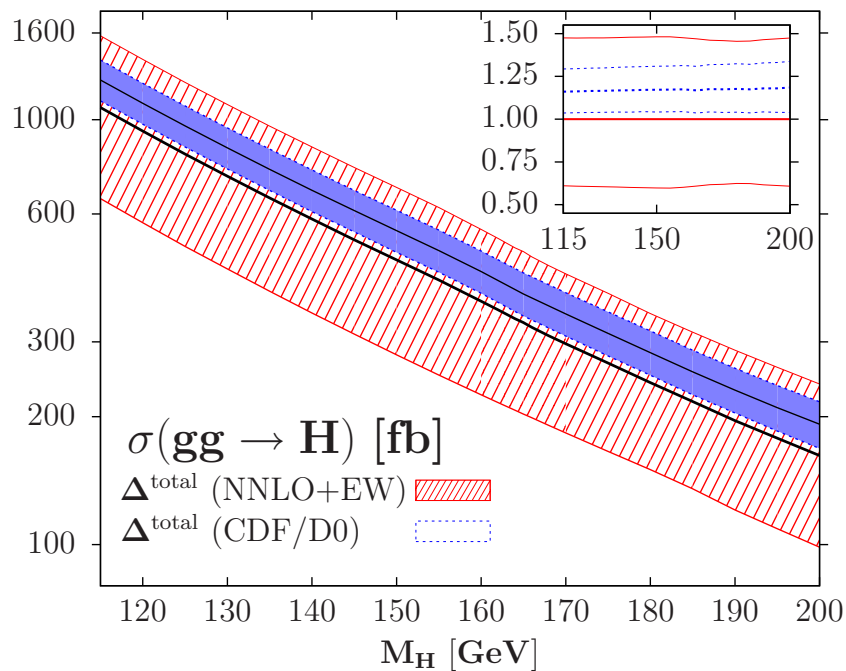


Figure 11. The production cross section $\sigma(gg \rightarrow H)$ at NNLO at the Tevatron with the uncertainty band when all the errors are added using our procedure (last columns of table 2). It is compared to $\sigma(gg \rightarrow H)$ at NNLL when the scale and PDF errors given in ref. [25] are added in quadrature. In the insert the relative deviations are shown when the central values are normalized to $\sigma^{\text{NNLO+EW}}$.

section that we obtain when including the higher order contributions only to NNLO and has a milder scale variation. As can be seen, the difference between the two uncertainty bands is striking. In fact, even the lower value of the cross section in the NNLL approach, including the scale and PDF errors when combined in quadrature, only touches the central value of our NNLO result. For $M_H = 160$ GeV, the lower value of the cross section, when all errors are included, is $\approx 40\%$ smaller than the central value at NNLO and $\approx 50\%$ smaller than the NNLL cross section adopted in ref. [8] as a normalisation.

We thus believe that the CDF/D0 combined analysis which rules out the 162–166 GeV mass range for the SM Higgs boson on the basis of the $gg \rightarrow H \rightarrow \ell\ell\nu\nu + X$ process, which is the most (if not the only) relevant one in this specific mass range at the Tevatron, has largely underestimated the theoretical errors on the Higgs production cross section. In fact, even if the scale uncertainty were taken to be that resulting from a variation in the usual domain $\frac{1}{2}M_H \leq \mu_F, \mu_R \leq 2M_H$ or the errors from the use of the effective approach at NNLO were ignored, the total uncertainty would have been of the order of $\approx 35\%$, i.e. three times larger than the error assumed in the CDF/D0 analysis.

Turning to the Higgs-strahlung processes, and similarly to the $gg \rightarrow H$ case, we display in table 3 the central values of the cross sections for $p\bar{p} \rightarrow WH$ and $p\bar{p} \rightarrow ZH$ at the Tevatron, evaluated at scales $\mu_R = \mu_F = M_{H_V}$ with the MSTW set of PDFs (second and third columns). In the remaining columns, we specialize in the WH channel and dis-

M_H	σ_{HW}	σ_{HZ}	scale	PDF	PDF+ α_s^{exp}	α_s^{th}	total	% total
115	174.5	103.9	+1.3 -1.6	+10.5 -9.1	+10.7 -10.7	+1.3 -0.9	+12.1 -12.3	+7% -7%
120	150.1	90.2	+1.1 -1.4	+9.2 -8.1	+9.6 -9.4	+1.2 -0.9	+10.7 -10.9	+7% -7%
125	129.5	78.5	+0.9 -1.3	+7.5 -6.8	+8.6 -8.7	+1.1 -0.8	+9.6 -10.0	+7% -8%
130	112.0	68.5	+0.8 -1.1	+6.8 -6.4	+7.2 -7.5	+1.1 -0.8	+8.0 -8.6	+7% -8%
135	97.2	60.0	+0.7 -1.0	+5.6 -5.5	+6.7 -6.6	+1.0 -0.7	+7.4 -7.6	+8% -8%
140	84.6	52.7	+0.6 -0.9	+5.6 -4.5	+5.8 -5.7	+0.9 -0.7	+6.5 -6.6	+8% -8%
145	73.7	46.3	+0.5 -0.8	+4.4 -4.1	+5.4 -5.2	+0.9 -0.7	+5.9 -6.0	+8% -8%
150	64.4	40.8	+0.5 -0.7	+4.2 -3.9	+4.4 -4.3	+0.8 -0.6	+5.0 -5.0	+8% -8%
155	56.2	35.9	+0.4 -0.6	+3.4 -3.1	+4.2 -4.1	+0.7 -0.6	+4.6 -4.7	+8% -8%
160	48.5	31.4	+0.4 -0.6	+3.3 -3.0	+3.6 -3.3	+0.7 -0.5	+4.1 -4.0	+8% -8%
162	47.0	30.6	+0.4 -0.5	+3.4 -2.8	+3.5 -3.3	+0.7 -0.5	+3.9 -3.8	+8% -8%
164	44.7	29.1	+0.3 -0.5	+3.1 -2.7	+3.4 -3.4	+0.6 -0.5	+3.7 -3.9	+8% -9%
165	43.6	28.4	+0.3 -0.5	+2.8 -2.4	+3.4 -3.3	+0.6 -0.5	+3.8 -3.8	+8% -8%
166	42.5	27.8	+0.3 -0.5	+3.0 -2.6	+3.1 -3.0	+0.6 -0.5	+3.4 -3.5	+8% -8%
168	40.4	26.5	+0.3 -0.5	+2.8 -2.4	+3.1 -2.9	+0.6 -0.5	+3.4 -3.4	+9% -8%
170	38.5	25.3	+0.3 -0.4	+2.9 -2.2	+3.0 -2.7	+0.6 -0.5	+3.3 -3.1	+9% -8%
175	34.0	22.5	+0.3 -0.4	+2.2 -1.9	+2.7 -2.6	+0.5 -0.4	+3.0 -3.0	+9% -9%
180	30.1	20.0	+0.2 -0.4	+2.1 -1.8	+2.2 -2.2	+0.5 -0.4	+2.5 -2.6	+8% -9%
185	26.9	17.9	+0.2 -0.3	+1.8 -1.5	+2.1 -2.1	+0.5 -0.4	+2.3 -2.4	+9% -9%
190	24.0	16.1	+0.2 -0.3	+1.6 -1.6	+1.8 -1.8	+0.4 -0.3	+2.1 -2.1	+9% -9%
195	21.4	14.4	+0.2 -0.3	+1.3 -1.2	+1.8 -1.7	+0.4 -0.3	+2.1 -2.0	+10% -10%
200	19.1	13.0	+0.2 -0.2	+1.4 -1.2	+1.5 -1.4	+0.4 -0.3	+1.8 -1.7	+9% -9%

Table 3. The central values of the cross sections for the $p\bar{p} \rightarrow WH$ and ZH processes at the Tevatron (in fb) for given Higgs mass values (in GeV) with, in the case of the WH channel, the uncertainties from scale variation, PDF, PDF+ $\Delta^{\text{exp}}\alpha_s$ and $\Delta^{\text{th}}\alpha_s$, as well as the total uncertainty when all errors are added using the procedure described in the text.

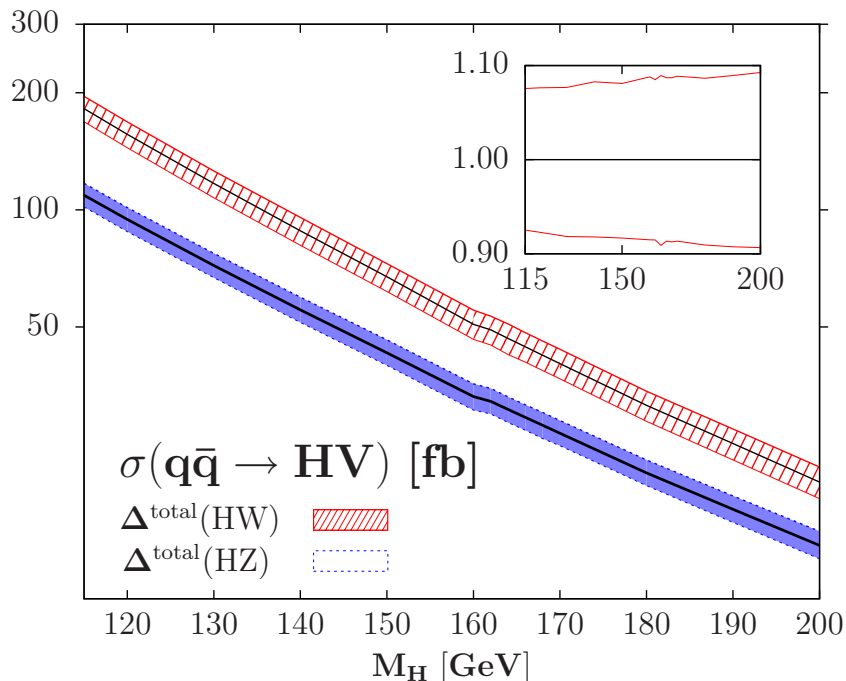


Figure 12. The production cross section $\sigma(p\bar{p} \rightarrow WH)$ and $\sigma(p\bar{p} \rightarrow ZH)$ at NNLO in QCD and electroweak NLO at the Tevatron evaluated with the MSTW set of PDFs, together with the uncertainty bands when all the theoretical errors are added. In the insert, the relative deviations from the central MSTW value are shown in the case of $\sigma(p\bar{p} \rightarrow WH)$.

play the errors from the scale variation (with $\kappa = 2$), the PDF, mixed PDF+ $\Delta^{\text{exp}}\alpha_s$ and PDF+ $\Delta^{\text{exp}}\alpha_s+\Delta^{\text{th}}\alpha_s$ uncertainties in the MSTW scheme. In the last columns, we give the total error and its percentage; this percentage error is, to a very good approximation, the same in the $p\bar{p} \rightarrow ZH$ channel. In contrast to the $g\bar{g} \rightarrow H$ mechanism, since the errors due to scale variation are rather moderate in this case, there is no large difference between the central cross section σ_0 and the cross sections $\sigma_0 \pm \Delta\sigma_\mu^\pm$ and, hence, the PDF, PDF+ $\Delta^{\text{exp}}\alpha_s$ and PDF+ $\Delta^{\text{exp}}\alpha_s+\Delta^{\text{th}}\alpha_s$ errors on σ^0 are, to a good approximation, the same as the errors on $\sigma_0 \pm \Delta\sigma_\mu^\pm$ displayed in table 3.

The total uncertainty is once more summarized in figure 12, where the cross sections for WH and ZH associated production at the Tevatron, together with the total uncertainty bands (in absolute values in the main frame and in percentage in the insert), are displayed as a function of the Higgs mass. As can be seen, the total error on the cross sections in the Higgs-strahlung processes is about $\pm 9\%$ in the entire Higgs mass range, possibly 1% to 2% smaller for low M_H values and $\sim 1\%$ larger for high M_H values. Thus, the theoretical errors are much smaller than in the case of the $g\bar{g} \rightarrow H$ process and the cross sections for the Higgs-strahlung processes are well under control. Nevertheless, the total uncertainty obtained in our analysis is almost twice as large as the total 5% uncertainty assumed by the CDF and D0 collaborations in their combined analysis of this channel [8].

Before closing this section, let us mention that the uncertainties in the Higgs-strahlung processes can be significantly reduced by using the Drell-Yan processes of massive gauge boson production as standard candles; a suggestion first made in ref., e.g. [120]. Indeed, normalizing the cross sections of associated WH and ZH production to the cross sections of single W and Z production, respectively, allows for a cancellation of several experimental errors such as the error on the luminosity measurement, as well as the partial cancellation (since the scales that are involved in the $p\bar{p} \rightarrow V$ and HV processes are different) theoretical errors such as those due to the PDFs, α_s and the higher order radiative corrections.

6 Conclusion

In the first part of this paper, we have evaluated the production cross sections of the Standard Model Higgs boson at the Tevatron, focusing on the two main channels: the gluon-gluon fusion $gg \rightarrow H$ mechanism that dominates in the high Higgs mass range and the Higgs-strahlung processes $q\bar{q} \rightarrow VH$ with $V = W, Z$, which are the most important ones in the lower Higgs mass range. In the determination of the cross sections, we have included all the available and relevant higher order corrections in perturbation theory, in particular, the QCD corrections up to NNLO and the one-loop electroweak radiative corrections. We have then provided up-to-date central values of the cross sections for the entire Higgs mass range that is relevant at the Tevatron. While this update has been performed for the $gg \rightarrow H$ mechanism in several recent analyses, it was missing in the case of the Higgs-strahlung processes.

The second part of the paper addresses the important issue of the theoretical uncertainties that affect the predicted cross sections. We have first discussed the scale uncertainties which are usually viewed as a measure of the unknown higher order contributions. Because the calculated QCD corrections are extremely large in the $gg \rightarrow H$ process, we point out that the domain of variation of the renormalisation and factorisation scales that is usually adopted in the literature should be extended. We adopt a criterion that allows for a more reasonable or conservative estimate of this variation domain: the range of variation of the scales at NNLO, should be the one which allows to the scale uncertainty band of the NLO cross section to include the NNLO contributions. Applying this criterion to the NNLO $gg \rightarrow H$ cross section and adopting a central scale $\mu_0 = M_H$, we obtain a scale uncertainty of the order of $\pm 20\%$, i.e. slightly larger than the $\approx \pm 15\%$ uncertainty that is usually assumed. This larger error would at least account for the 20–30% discrepancy between the QCD corrections to the inclusive cross section that is used as a normalisation and the cross section with the basic kinematical cuts applied in the experimental analyses.

A second source of uncertainties in the $gg \rightarrow H$ cross section originates from the use of the effective theory approach that allows to considerably simplify the calculation of the NNLO contributions, an approach in which the masses of the loop particles that generate the Hgg vertex are assumed to be much larger than the Higgs mass. We show that the missing NNLO contribution of the b -quark loop where the limit $M_H \ll m_b$ cannot be applied (together with the definition of the b -quark mass), and the approximation $M_H \ll M_W$

used in the three-loop mixed QCD-electroweak NNLO radiative corrections, might lead to a few percent error on the total $gg \rightarrow H$ cross section in each case.

A third source of theoretical errors is due to the parton distribution functions and the errors associated to the strong coupling constant. Considering not only the MSTW scheme as usually done, but also the CTEQ and ABKM schemes, we recall that while the PDF errors are relatively small within a given scheme, the central values can be widely different. This is particularly true in the case of the $gg \rightarrow H$ cross section, where the central values in the MSTW/CTEQ and ABKM schemes differ by about 25%. Only when the experimental as well as the theoretical errors on α_s are accounted for that one obtains results that are consistent when using the MSTW/CTEQ and ABKM schemes. In the MSTW scheme, using a recently released set-up which provides a simultaneous access to the PDF and $\Delta^{\text{exp}}\alpha_s$ errors as well as a way to estimate the $\Delta^{\text{th}}\alpha_s$ error, one finds a $\approx 15\%$ uncertainty on $\sigma(gg \rightarrow H)$, that is, at least a factor of two larger than the uncertainty due to the PDFs alone that is usually considered as the total PDF error

We have then proposed a simple procedure to combine these various theoretical errors. The main idea of this procedure is to evaluate directly the PDF+ $\Delta^{\text{exp}}\alpha_s+\Delta^{\text{th}}\alpha_s$ error, as well as the significantly smaller errors due to the use of the effective approach in the $gg \rightarrow H$ process at NNLO, on the maximal and minimal values of the cross sections that one obtains when varying the renormalisation and factorisation scales in the chosen domain.

Adopting this approach, one arrives at a total uncertainty of $\approx -40\%$ and $\approx +50\%$ for the central value of the $gg \rightarrow H$ cross section at the Tevatron, a much larger error than the $\approx 10\%$ uncertainty that is usually assumed.²¹ Hence, the number of signal events from the $gg \rightarrow H$ process with the subsequent Higgs decay $H \rightarrow WW \rightarrow \ell\nu\nu$, i.e. the main (if not the only relevant) Higgs channel at the Tevatron in the Higgs mass range $150 \text{ GeV} \lesssim M_H \lesssim 180 \text{ GeV}$, might be a factor of two smaller than what has been assumed by the CDF and D0 collaborations in their recent analysis which excluded the Higgs mass range between 162 and 166 GeV. We thus believe that this analysis should be reconsidered in the light of these larger theoretical uncertainties in the signal cross sections.²²

Of course, one can view the results presented in this paper with a more optimistic perspective: since the uncertainties in the $gg \rightarrow H$ process are so large, the cross section might well be closer to its upper limit which is $\approx 50\%$ higher than the central value. In this lucky situation, the sensitivities of the CDF and D0 collaborations would be significantly

²¹We note that it would be interesting to study the impact of these theoretical uncertainties on the $gg \rightarrow H$ cross sections for Higgs production at the LHC, not only for the discovery of the particle, but also for the measurement of its couplings to fermions and gauge bosons, see for instance [121–123], which is another crucial issue in this context. A preliminary analysis shows that at $\sqrt{s} = 14 \text{ TeV}$, the total error that one obtains on the NNLO total production cross section is of the order of 25% for $M_H \approx 160 \text{ GeV}$, i.e. much less than at the Tevatron. The main reason is that the PDF+ α_s uncertainties are slightly smaller than those obtained for the Tevatron, while the scale uncertainty (in which one needs only the more reasonable factor $\kappa = 2$) is reduced, $\lesssim 15\%$, a mere consequence of the fact that the K -factors are more moderate, $K_{\text{NNLO}} \approx 2$ at the LHC instead of $K_{\text{NNLO}} \approx 3$ at the Tevatron. More details will be given elsewhere [124].

²²This is without considering the uncertainties in the background cross sections. It would be indeed interesting to apply our procedure for the evaluation of the scale variation, the PDF+ α_s errors and for their combination, to the major expected backgrounds of the Higgs signal, namely Drell-Yan, top quark pair and gauge boson pair production. This is, however, beyond the scope of the present paper.

increased and if the Higgs boson happens to have a mass in the range $M_H \approx 160\text{--}170$ GeV, some evidence for the particle at the Tevatron might soon show up.

Finally, in the case of the Higgs-strahlung processes, the cross sections are much more under control, the main reason being due to the fact that the QCD corrections are moderate. The scale uncertainties are at percent level for the narrow domain chosen for the scale variation (within a factor of two from the central scale), while the PDF uncertainties and the associated uncertainties due to the experimental and theoretical errors on α_s are much smaller than in the $gg \rightarrow H$ case. The total estimated theoretical error on the Higgs-strahlung cross sections, $\approx 10\%$, is nevertheless almost twice as large as the error assumed by the CDF and D0 collaborations.

Acknowledgments

This work is supported by the European network HEPTOOLS. JB thanks the CERN TH group for the hospitality extended to him during this work. Discussions with Babis Anastasiou, Michael Dittmar, Davide Gerbaudo, Massimiliano Grazzini, Wade Fisher, Robert Harlander, Vajravelu Ravindran, Peter Skands, Michael Spira and Peter Uwer are gratefully acknowledged. Special thanks go to Michael Spira for his critical comments on an earlier version of the manuscript.

7 Addendum

After our paper appeared on the archives, some criticisms have been made by the members of the Tevatron New Physics and Higgs working group (TevNPHWG) of the CDF and D0 collaborations [125] concerning the theoretical modeling of the $gg \rightarrow H$ production cross section that we proposed. This criticism appeared on the web in May 2010, but we got aware of it only during ICHEP, i.e. end of July 2010, where, incidentally, the new combined analysis of CDF and D0 for the Higgs search at the Tevatron was released [126, 127]. In this addendum, we respond to this criticism point by point and, in particular, perform a new analysis of the $gg \rightarrow H$ cross section at NNLO for a central value of the renormalization and factorization scales $\mu_0 = \frac{1}{2}M_H$, for which higher order corrections beyond NNLO (that we discarded with some justification in our previous analysis) are implicitly included. We take the opportunity to also comment on the new CDF/D0 results with which the excluded Higgs mass range was extended to $M_H = 158\text{--}175$ GeV at the 95% CL.²³

7.1 The normalization of the $gg \rightarrow H$ cross section

One of the points put forward in our paper is to suggest to consider the $gg \rightarrow H$ production cross section up to NNLO $\sigma_{gg \rightarrow H}^{\text{NNLO}}$, and not to include the soft-gluon resummation contributions. The main reason is that, ultimately, the observable that is experimentally used is the cross section $\sigma_{gg \rightarrow H}^{\text{cuts}}$ in which selection cuts have been applied and the theoretical

²³Some of the points that we discuss here have also been presented by one of us (JB) in the Higgs Hunting workshop in Orsay which followed ICHEP (*Higgs Hunting workshop*, held in Orsay France July 29–31 2010, <http://indico.lal.in2p3.fr/conferenceDisplay.py?confid=1109>).

prediction for $\sigma_{gg \rightarrow H}^{\text{cuts}}$ is available only to NNLO, This argument has been criticized by the TevNPHWG for the reason that we are potentially missing some important higher order contributions to the cross section. It turns out, however, that our point is strengthened in the light of the new CDF/D0 combined analysis [126, 127]. Indeed, in this analysis, the $gg \rightarrow H$ cross section has been broken into the three pieces which yield different final state signal topologies for the main decay $H \rightarrow WW^{(*0)} \rightarrow \ell\nu\nu$, namely $\ell\nu\nu+0\text{jet}$, $\ell\nu\nu+1\text{jet}$ and $\ell\nu\nu+2\text{jets}$ or more:

$$\sigma_{gg \rightarrow H}^{\text{NNLO}} = \sigma_{gg \rightarrow H}^{0\text{jet}} + \sigma_{gg \rightarrow H}^{1\text{jet}} + \sigma_{gg \rightarrow H}^{\geq 2\text{jets}} \quad (7.1)$$

These channels have been analyzed separately and these individual components, with $\sigma_{gg \rightarrow H}^{0\text{jet}}$ evaluated at NNLO, $\sigma_{gg \rightarrow H}^{1\text{jet}}$ evaluated at NLO and $\sigma_{gg \rightarrow H}^{\geq 2\text{jets}}$ evaluated at LO, represent respectively $\approx 60\%$, $\approx 30\%$ and $\approx 10\%$ of the total $gg \rightarrow H$ cross section at NNLO. Since these three pieces add up to $\sigma_{gg \rightarrow H}^{\text{NNLO}}$, we do not find appropriate to have a different normalization for the jet cross sections and for the total sum and, thus, to include soft-gluon resummation in the latter while it is not taken into account in the former.

Nevertheless, we are ready to admit that we may have underestimated the total production cross section, as with the central value of the renormalization and factorization scales $\mu_R = \mu_F = \mu_0 = M_H$ that we have adopted for evaluating $\sigma_{gg \rightarrow H}^{\text{NNLO}}$, we are missing the $\gtrsim 10\%$ increase of the cross section due to higher order contributions and, in particular, to soft-gluon resummation. As most criticism on our paper focused on this particular issue (overlooking many other points that we put forward), we present here an analysis of the cross section in which these higher order effects are implicitly taken into account.

As pointed out by Anastasiou and collaborators some time ago, see e.g. refs. [27, 128] (and also ref. [5]), the effects of soft-gluon resummation at NNLL [24] can be accounted for in $\sigma_{gg \rightarrow H}^{\text{NNLO}}$ by lowering the central value of the renormalization and factorization scales²⁴ from $\mu_0 = M_H$ to $\mu_0 = \frac{1}{2}M_H$. If the scale value $\mu_0 = \frac{1}{2}M_H$ is chosen, the central value of $\sigma_{gg \rightarrow H}^{\text{NNLO}}$ increases by more than 10% and there is almost no difference between $\sigma_{gg \rightarrow H}^{\text{NNLO}}(\mu_0 = \frac{1}{2}M_H)$ and $\sigma_{gg \rightarrow H}^{\text{NNLL}}(\mu_0 = M_H)$ as calculated for instance by de Florian and Grazzini [25].

This is explicitly shown in figure 13 where $\sigma_{gg \rightarrow H}^{\text{NNLO}}$ with central scales $\mu_0 = M_H$ and $\mu_0 = \frac{1}{2}M_H$ (that we calculate following the same lines as the ones discussed in section 2 of our paper) are compared to $\sigma_{gg \rightarrow H}^{\text{NNLL}}$ with $\mu_0 = M_H$ (for which the numbers are given in ref. [25]). For instance, for $M_H \approx 160\text{ GeV}$, while there is a $\simeq 14\%$ difference between $\sigma_{gg \rightarrow H}^{\text{NNLO}}(\mu_0 = M_H)$ and $\sigma_{gg \rightarrow H}^{\text{NNLL}}(\mu_0 = M_H)$, there is almost no difference between the later and $\sigma_{gg \rightarrow H}^{\text{NNLO}}(\mu_0 = \frac{1}{2}M_H)$.

As a result of this choice, our normalization for the inclusive cross section is now the same as the ones of refs. [25, 27] which were adopted in the combined CDF/D0 analyses.

7.2 The scale uncertainty

The next important issue is the range of variation that one should adopt for the renormalization and factorization scales, a variation which leads to an uncertainty band that is

²⁴Note that the scale choice $\mu_0 = \frac{1}{2}M_H$ in $gg \rightarrow H$ does not only mimic the inclusion of the effect of soft-gluon resummation, but it also improves the convergence of the perturbative series and is more appropriate to describe the kinematics of the process [128].

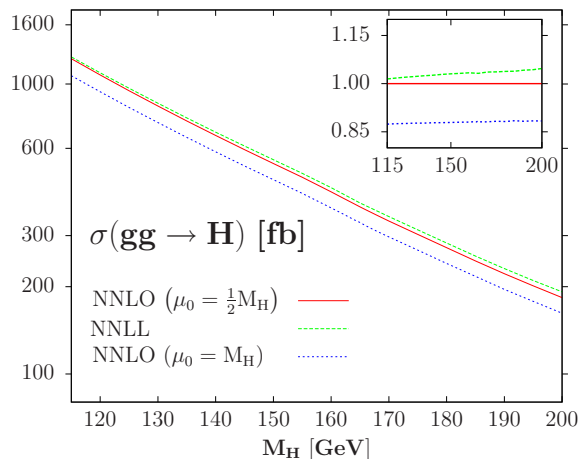


Figure 13. The $gg \rightarrow H$ cross section at the Tevatron as a function of M_H : at NNLO for central scales at $\mu_0 = M_H$ and $\mu_0 = \frac{1}{2}M_H$ and at NNLL for a scale $\mu_0 = M_H$. In the insert, shown are the deviations when one normalizes to $\sigma_{gg \rightarrow H}^{\text{NNLO}}(\mu_0 = \frac{1}{2}M_H)$.

supposed to be a measure of the unknown (not yet calculated) higher order contributions to the cross section. In our paper, we have advocated the fact that since the NLO and NNLO QCD corrections in the $gg \rightarrow H$ process were so large, it is wiser to extend the range of scale variation from what is usually assumed. From the requirement that the scale variation of the LO or NLO cross sections around the central scale μ_0 catch the central value of $\sigma_{gg \rightarrow H}^{\text{NNLO}}$, we arrived at the minimal choice, $\frac{1}{3}\mu_0 \leq \mu_R, \mu_F \leq 3\mu_0$ for $\mu_0 = M_H$.

In addition, we proposed that the scales μ_R and μ_F are varied independently and with no restriction such as $\frac{1}{3} \leq \mu_R/\mu_F \leq 3$ for instance. In fact, this was only a general statement and this requirement had absolutely no impact on our analysis as the minimal and maximal values of $\sigma_{gg \rightarrow H}^{\text{NNLO}}$ due to scale variation were obtained for equal μ_R and μ_F values: for a central scale $\mu_0 = M_H$, one had $\sigma_{\text{min}}^{\text{NNLO}}$ for $\mu_R = \mu_F = 3\mu_0$ and $\sigma_{\text{max}}^{\text{NNLO}}$ for $\mu_R = \mu_F = \frac{1}{3}\mu_0$.

Adopting the central scale choice $\mu_0 = \frac{1}{2}M_H$, for the scale variation of the leading-order $gg \rightarrow H$ cross section to catch the central value of $\sigma_{gg \rightarrow H}^{\text{NNLO}}(\mu_0)$, as shown in the left-hand side of figure 14, we again need to consider the domain

$$\frac{1}{3}\mu_0 \leq \mu_R = \mu_F \leq 3\mu_0, \quad \mu_0 = \frac{1}{2}M_H \tag{7.2}$$

for the scale variation. Notice that now, we choose for simplicity to equate μ_R and μ_F so that there is no more discussion about the possibility of generating artificially large logarithms if we take two widely different μ_R/μ_F scales.

Adopting this domain for $\mu_F = \mu_R$, we obtain the result shown in the right-hand side of figure 14 for the scale variation of the NNLO cross section around the central scale $\mu_0 = \frac{1}{2}M_H$. Averaged over the entire Higgs mass range, the final scale uncertainty is about $\simeq +15\%, -20\%$ which, compared with our previous result for the scale variation of $\sigma_{gg \rightarrow H}^{\text{NNLO}}$ with $\mu_0 = M_H$ is the same for the minimal value but smaller for the maximal value. Note that if we had chosen the usual domain $\frac{1}{2}\mu_0 \leq \mu_R = \mu_F \leq 2\mu_0$, the scale variation would have been of about $\approx +10\%, -12\%$ for $M_H \approx 160$ GeV.

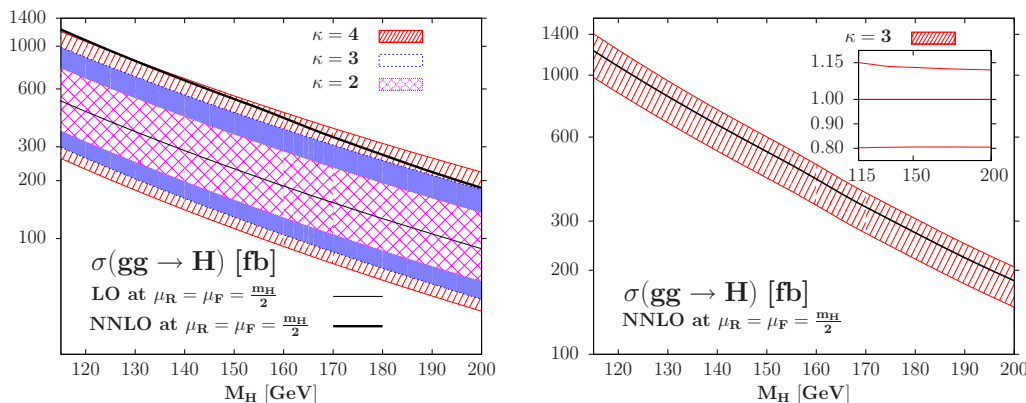


Figure 14. Left: the scale variation of $\sigma_{gg \rightarrow H}^{\text{LO}}$ as a function of M_H in the domain $\mu_0/\kappa \leq \mu_R = \mu_F \leq \kappa\mu_0$ for $\mu_0 = \frac{1}{2}M_H$ with $\kappa = 2, 3$ and 4 compared to $\sigma_{gg \rightarrow H}^{\text{NNLO}}(\mu_R = \mu_F = \frac{1}{2}M_H)$. Right: the uncertainty band of $\sigma_{gg \rightarrow H}^{\text{NNLO}}$ as a function of M_H for a scale variation $\mu_0/\kappa \leq \mu_R = \mu_F \leq \kappa\mu_0$ with $\mu_0 = \frac{1}{2}M_H$ and $\kappa = 3$. In the inserts shown are the relative deviations.

It is important to notice that if the NNLO $gg \rightarrow H$ cross section, evaluated at $\mu_0 = M_H$, is broken into the three pieces with 0,1 and 2 jets, and one applies a scale variation for the individual pieces in the range $\frac{1}{2}\mu_0 \leq \mu_R, \mu_F \leq 2\mu_0$, one obtains with selection cuts similar to those adopted by the CDF/D0 collaborations [26]:

$$\Delta\sigma/\sigma|_{\text{scale}} = 60\% \cdot \begin{pmatrix} +5\% \\ -9\% \end{pmatrix} + 29\% \cdot \begin{pmatrix} +24\% \\ -23\% \end{pmatrix} + 11\% \cdot \begin{pmatrix} +91\% \\ -44\% \end{pmatrix} = \begin{pmatrix} +20.0\% \\ -16.9\% \end{pmatrix} \quad (7.3)$$

Averaged over the various final states with their corresponding weights, an error on the “inclusive” cross section which is about $+20\%$, -17% is derived.²⁵ This is very close to the result obtained in the CDF/D0 analysis [126, 127] which quotes a scale uncertainty of $\approx \pm 17.5\%$ on the total cross section, when the weighted uncertainties for the various jet cross sections are added. Thus, our supposedly “conservative” choice $\frac{1}{3}\mu_0 \leq \mu_R = \mu_F \leq 3\mu_0$ for the scale variation of the total inclusive cross section $\sigma_{\text{gg} \rightarrow \text{H}}^{\text{NNLO}}$, leads to a scale uncertainty that is very close to that obtained when one adds the scale uncertainties of the various jet cross sections for a variation around the more “consensual” range $\frac{1}{2}\mu_0 \leq \mu_R, \mu_F \leq 2\mu_0$.

We also note that when breaking $\sigma_{\text{gg} \rightarrow \text{H}}^{\text{NNLO}}$ into jet cross sections, an additional error due to the acceptance of jets is introduced; the CDF and D0 collaborations, after weighting, have estimated it to be $\pm 7.5\%$. We do not know if this weighted acceptance error should be considered as a theoretical or an experimental uncertainty. But this error, combined with the weighted uncertainty for scale variation, will certainly increase the total scale error in the CDF/D0 analysis, possibly (and depending on how the errors should be added) to the level where it almost reaches or even exceeds our own supposedly “conservative” estimate.

7.3 PDF and α_s uncertainties

Another issue is the uncertainties due to the parameterization of the PDFs and the corresponding ones from the value of the strong coupling constant α_s . In their updated

²⁵The error might be reduced when including higher-order corrections in the 1 jet and 2 jet cross sections.

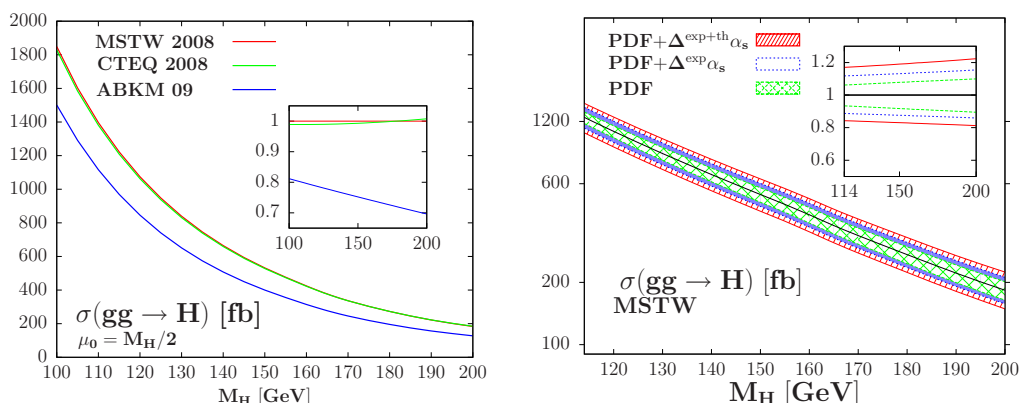


Figure 15. Left: the $gg \rightarrow H$ cross section at NNLO for $\mu_0 = \frac{1}{2}M_H$ as a function of M_H when the MSTW, CTEQ and ABKM parameterizations are used. Left: the 90%CL PDF, PDF+ $\Delta^{\text{exp}}\alpha_s$ and PDF+ $\Delta^{\text{exp+th}}\alpha_s$ uncertainties on $\sigma_{gg \rightarrow H}^{\text{NNLO}}$ in the MSTW parametrisation. In the inserts, shown in % are the deviations with respect to the central MSTW value.

analysis [126, 127], the CDF and D0 collaborations are now including the uncertainties generated by the experimental error in the value of α_s and considering the PDF+ $\Delta^{\text{exp}}\alpha_s$ uncertainty, but there is still a little way to go as the problem of the theoretical error on α_s is still pending.

For the new analysis that we present here for $\sigma_{gg \rightarrow H}^{\text{NNLO}}$ with a central scale $\mu_0 = \frac{1}{2}M_H$, we have only slightly changed our previous recipe for calculating the errors due to PDFs and α_s : we still use the grids provided by the MSTW collaboration [42, 43] for PDF+ $\Delta^{\text{exp}}\alpha_s$, take the 90%CL result and add in quadrature the impact of the theoretical error $\Delta^{\text{th}}\alpha_s$ using again the sets provided by the MSTW collaboration. However, contrary to the case $\mu_0 = M_H$ where the value $\Delta^{\text{th}}\alpha_s = 0.003$ at NLO ($\Delta^{\text{th}}\alpha_s = 0.002$ at NNLO) as suggested by MSTW [42, 43] was sufficient to achieve a partial overlap of the MSTW and ABKM predictions (which, together with the CTEQ prediction, are given in the left-hand side of figure 15) when including their respective error bands, we need in the case $\mu_0 = \frac{1}{2}M_H$ an uncertainty of $\Delta^{\text{th}}\alpha_s = 0.004$, to make such that the MSTW and ABKM predictions, which differ by more than 25% in this case, become consistent.

Adopting this value for the α_s theoretical uncertainty, which is approximately the difference between the MSTW and ABKM central α_s values, the results for $\sigma_{gg \rightarrow H}^{\text{NNLO}}$ using only the MSTW parametrisation are displayed in the right-hand side of figure 15. Shown are the 90% confidence level PDF, PDF+ $\Delta^{\text{exp}}\alpha_s$ and PDF+ $\Delta^{\text{exp+th}}\alpha_s$ uncertainties, with the PDF+ $\Delta^{\text{exp}}\alpha_s$ and PDF+ $\Delta^{\text{th}}\alpha_s$ combined in quadrature. We thus obtain a PDF+ $\Delta^{\text{exp+th}}\alpha_s$ total uncertainty of $\pm 15\%$ to 20% on the central cross section depending on the M_H value. This is larger than the 12.5% error which has been assumed in the most recent CDF/D0 combined analysis [126, 127] (and even larger than the $\approx \pm 8\%$ assumed in the earlier analysis [7]). We believe that if the effect of the theoretical error on α_s is taken into account in the Tevatron analysis of $\sigma(gg \rightarrow H)$, we will arrive at a much closer agreement.

We would like to insist on the fact that this recipe is only one particular way, and by no means the only one, of parameterizing the PDF uncertainty. A possibly more adequate procedure to evaluate this theoretical uncertainty would be to consider the difference between the central values given by various PDF sets. In the present $gg \rightarrow H$ case, while the MSTW and CTEQ parameterizations give approximately the same result as shown previously, ABKM gives a central NNLO cross section that is $\approx 25\%$ smaller than that obtained using the MSTW set.²⁶ The PDF uncertainty, in this case, would be thus $\approx -25\%, +0\%$.

We also note that there is another recipe that has been suggested by the PDF@LHC working group for evaluating PDF uncertainties for NNLO cross sections (besides taking the envelope of the predicted values obtained using several PDF sets) [129]: take the MSTW PDF $+\Delta^{\text{exp}}\alpha_s$ error and multiply it by a factor of two. In our case, this would lead to an uncertainty of $\approx \pm 25\%$ which, for the minimal value, is close to the recipe discussed just above, and is larger than what we obtain when considering the PDF $+\Delta^{\text{exp+th}}\alpha_s$ uncertainty given by MSTW. We thus believe that our estimate of the PDF $+\alpha_s$ uncertainty that we quote here is far from being exaggeratedly conservative.

7.4 Combination of the various uncertainties

The last issue that remains to be discussed and which, to our opinion is the main one, is the way of combining the various sources of theoretical errors. Let us first reiterate an important comment: the uncertainties associated to the PDF parameterisations are theoretical errors and they have been considered as such since a long time. Indeed, although the PDF sets use various experimental data which have intrinsic errors (and which are at the origin of the misleading “probabilistic” interpretation of the errors given by each PDF set that are generally quoted), the main uncertainty is due to the theoretical assumptions which go into the different parameterizations. This uncertainty cannot be easily quantified within one given parametrisation but it is reflected in the spread of the central values given by the various PDF parameterizations that are available. If one defines the PDF uncertainty as the difference in the cross sections when using the different available PDF sets, this uncertainty has no statistical or probabilistic ground. For the scale uncertainty, the situation is of course clear: it has no statistical ground and any value of the cross section in the uncertainty band is as respectable as another.²⁷

As a result, the scale and PDF uncertainties, cannot be combined in quadrature as done, for instance, by the CDF and D0 collaborations. This is especially true as in the $gg \rightarrow H$ process, a strong correlation between the renormalization and factorization scales that are involved (and that we have equated here for simplicity, $\mu_R = \mu_F$), the value of α_s and the gg densities is present. For instance, decreasing (increasing) the scales will increase (decrease) the $gg \rightarrow H$ cross section not only because of the lower (higher) $\alpha_s(\mu_R^2)$ value that is obtained and which decreases (increases) the magnitude of the matrix element squared (that is proportional to α_s^2 at leading order and the cross section is mini-

²⁶The $gg \rightarrow H$ cross section is even smaller if one uses the new NNLO central PDF sets recently released by the HERAPDF collaboration [130] rather than the ABKM PDF set.

²⁷In statistical language, both the scale and PDF uncertainties have a flat prior. A more elaborated discussion on this issue will appear in a separate publication [124].

mal/maximal for the highest/lowest $\mu_R = \mu_F$ values), but also because at the same time, the gg densities become smaller (larger) for higher (smaller) $\mu_F = \sqrt{Q^2}$ values [129].

Thus, not only the scale and PDF uncertainties cannot be added in quadrature, they also cannot be added linearly because of the aforementioned correlation. We therefore strongly believe that the best and safest procedure to combine the scale and PDF+ α_s uncertainties is the one proposed in our paper, that is, to estimate directly the PDF+ α_s uncertainties on the maximum/minimum cross sections with respect to the scale variation.

In addition, there is a last theoretical error which should be included, related to the use of the EFT approach for the b -quark loop at NNLO QCD (together with the parametric and scheme uncertainty on the b -quark mass) and for the electroweak radiative corrections, which amount to a few %. These uncertainties, discussed in detail in section 3.2, are also purely theoretical uncertainties and should be added linearly to the combined scale and PDF+ α_s uncertainty (as there is no apparent correlation between them).

Doing so for the $gg \rightarrow H$ NNLO cross section with a central scale $\mu_0 = \frac{1}{2}M_H$, we obtain the total error shown in figure 16, that we compare to the $\approx \pm 22\%$ error assumed in the CDF/D0 analysis. For $M_H = 160$ GeV for instance, we obtain $\Delta\sigma/\sigma \approx +41\%, -37\%$. Compared to our previous result with a central scale $\mu_0 = M_H$ which amounted to $\Delta\sigma/\sigma \simeq +48\%, -40\%$, this is approximately the same (only a few percent less) for the lower value of the cross section and significantly less for its upper value.

Hence, our procedure for the combination does not reduce to a linear sum of all uncertainties. If we had added linearly all errors, we would have had, for the negative part at $M_H = 160$ GeV, a total uncertainty of $\Delta\sigma/\sigma \approx -42\%$, compared to the value -37% with our procedure. On the other hand, one has an error of $\approx -30\%$, i.e. close to the total error assumed by CDF/D0 if the scale and PDF+ α_s uncertainties were added in quadrature and the EFT approach error linearly (the latter being ignored by the CDF/D0 collaborations).

7.5 Summary

We have updated our analysis on the theoretical predictions for the Higgs production cross section in the $gg \rightarrow H$ process at the Tevatron, by assuming a central scale $\mu_R = \mu_F = \mu_0 = \frac{1}{2}M_H$ which seems more appropriate to describe the process and implicitly accounts for the bulk of the higher order contributions beyond NNLO. We have then estimated the theoretical uncertainties associated to the prediction: the scale uncertainty, the uncertainties from the PDF parametrisation and the associated error on α_s , as well as uncertainties due to the use of the EFT approach for the mixed QCD-electroweak radiative corrections and the b -quark loop contribution. In table 4, we summarise the results that we have obtained: the first column shows the central cross section obtained at NNLO with $\mu_0 = \frac{1}{2}M_H$ and the other columns the individual uncertainties and the total absolute and relative uncertainties when the latter are combined using our procedure.

While our central value agrees now with the ones given in refs. [25, 27] and adopted by the CDF/D0 collaborations, the overall theoretical uncertainty that we obtain is approximately twice the error assumed in the latest Tevatron analysis to obtain the exclusion band $158 \text{ GeV} \leq M_H \leq 175 \text{ GeV}$ on the Higgs mass [126, 127]. This is a mere consequence of the different ways to combine the individual scale and PDF+ α_s uncertainties and, to a lesser

M_H	$\sigma_{gg \rightarrow H}^{\text{NNLO}}$ [fb]	scale	PDF	PDF+ α_s^{exp}	α_s^{th}	EW	b-loop	total	% total
100	1849	+318 -371	+102 -109	+210 -201	+219 -199	+45 -45	+42 -42	+817 -648	+44.2% -35.0%
105	1603	+262 -320	+91 -98	+184 -176	+192 -174	+41 -41	+39 -39	+700 -565	+43.7% -35.3%
110	1397	+219 -277	+83 -89	+163 -156	+170 -152	+37 -37	+35 -35	+602 -496	+43.1% -35.5%
115	1222	+183 -242	+75 -81	+144 -138	+151 -134	+33 -33	+32 -32	+521 -437	+42.6% -35.7%
120	1074	+156 -211	+69 -73	+129 -123	+135 -119	+30 -30	+29 -29	+454 -386	+42.2% -36.0%
125	948	+134 -186	+63 -67	+115 -110	+121 -106	+28 -28	+24 -24	+397 -342	+41.9% -36.1%
130	839	+115 -164	+57 -61	+104 -99	+108 -94	+25 -25	+21 -21	+349 -304	+41.5% -36.2%
135	746	+100 -145	+53 -56	+94 -89	+98 -84	+23 -23	+18 -18	+309 -272	+41.4% -36.5%
140	665	+88 -129	+48 -51	+85 -80	+88 -76	+21 -21	+16 -16	+275 -243	+41.4% -36.6%
145	594	+78 -115	+45 -47	+77 -73	+80 -68	+19 -19	+14 -14	+246 -218	+41.4% -36.8%
150	532	+69 -103	+41 -44	+70 -66	+73 -61	+17 -17	+13 -13	+221 -197	+41.6% -37.0%
155	477	+61 -92	+38 -40	+64 -60	+67 -55	+15 -15	+10 -10	+198 -176	+41.5% -37.0%
160	425	+54 -82	+35 -37	+58 -54	+60 -50	+11 -11	+9 -9	+175 -155	+41.3% -36.6%
162	405	+51 -78	+33 -35	+56 -52	+58 -48	+9 -9	+8 -8	+166 -146	+40.9% -36.2%
164	386	+48 -75	+32 -34	+53 -50	+55 -45	+8 -8	+8 -8	+158 -139	+40.9% -36.0%
165	377	+47 -73	+31 -33	+52 -48	+54 -44	+7 -7	+8 -8	+154 -135	+40.8% -35.9%
166	368	+46 -71	+31 -33	+51 -47	+53 -44	+6 -6	+8 -8	+150 -132	+40.9% -35.8%
168	352	+44 -68	+30 -31	+49 -46	+51 -42	+5 -5	+8 -8	+144 -126	+40.9% -35.7%
170	337	+42 -65	+29 -30	+47 -44	+49 -40	+4 -4	+7 -7	+137 -119	+40.6% -35.4%
175	303	+37 -59	+26 -28	+43 -40	+45 -36	+2 -2	+6 -6	+122 -106	+40.4% -35.1%
180	273	+33 -53	+24 -26	+39 -36	+41 -33	+1 -1	+6 -6	+111 -95	+40.6% -34.9%
185	245	+30 -47	+22 -24	+36 -33	+38 -30	+1 -1	+6 -6	+101 -87	+41.1% -35.3%
190	222	+27 -43	+21 -22	+33 -30	+35 -27	+2 -2	+5 -5	+92 -79	+41.4% -35.7%
195	201	+24 -39	+19 -20	+31 -28	+32 -25	+2 -2	+3 -3	+83 -72	+41.4% -35.8%
200	183	+22 -35	+18 -19	+28 -26	+30 -23	+2 -2	+3 -3	+77 -67	+42.0% -36.3%

Table 4. The NNLO total Higgs production cross sections in the $gg \rightarrow H$ process at the Tevatron (in fb) for given Higgs mass values (in GeV) at a central scale $\mu_F = \mu_R = \frac{1}{2}M_H$. Shown also are the corresponding shifts due to the theoretical uncertainties from the various sources discussed, as well as the total uncertainty when all errors are added using the procedure described in the text.

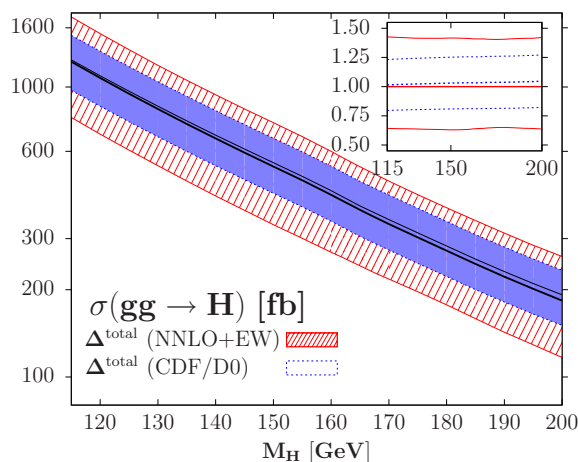


Figure 16. The production cross section $\sigma(gg \rightarrow H)$ at NNLO for the QCD and NLO for the electroweak corrections at the Tevatron at a central scale $\mu_F = \mu_R = \frac{1}{2}M_H$ with the uncertainty band when all theoretical uncertainties are added using our procedure. It is compared to $\sigma(gg \rightarrow H)$ at NNLL [25] with the errors quoted by the CDF/D0 collaboration [126, 127]. In the insert, the relative deviations compared to the central value are shown.

extent, the impact on the theoretical uncertainty on α_s and the EFT uncertainties which have not been considered by the CDF/D0 collaborations. We have provided arguments in favor of our procedure to combine the scale and PDF uncertainties and we therefore still believe that the CDF/D0 exclusion limit on the Higgs mass should be reconsidered.

Open Access. This article is distributed under the terms of the Creative Commons Attribution Noncommercial License which permits any noncommercial use, distribution, and reproduction in any medium, provided the original author(s) and source are credited.

References

- [1] P.W. Higgs, *Broken symmetries, massless particles and gauge fields*, *Phys. Lett.* **12** (1964) 132 [SPIRES].
- [2] F. Englert and R. Brout, *Broken symmetry and the mass of gauge vector mesons*, *Phys. Rev. Lett.* **13** (1964) 321 [SPIRES].
- [3] G.S. Guralnik, C.R. Hagen and T.W.B. Kibble, *Global conservation laws and massless particles*, *Phys. Rev. Lett.* **13** (1964) 585 [SPIRES].
- [4] P.W. Higgs, *Spontaneous symmetry breakdown without massless bosons*, *Phys. Rev.* **145** (1966) 1156 [SPIRES].
- [5] A. Djouadi, *The anatomy of electro-weak symmetry breaking. I: the Higgs boson in the standard model*, *Phys. Rept.* **457** (2008) 1 [hep-ph/0503172] [SPIRES].
- [6] *CERN bulletin*, issue No. 49-50/2009, Cern, Geneva Switzerland (2009) <http://cdsweb.cern.ch/journal/CERNBulletin/2009/49/News%20Articles/?ln=en>.

- [7] CDF AND D0 collaboration, T. Aaltonen et al., *Combination of Tevatron searches for the standard model Higgs boson in the W^+W^- decay mode*, *Phys. Rev. Lett.* **104** (2010) 061802 [[arXiv:1001.4162](#)] [[SPIRES](#)].
- [8] TEVNP WORKING GROUP collaboration for CDF AND D0 collaboration, *Combined CDF and D0 upper limits on standard model Higgs-boson production with 2.1–5.4 fb⁻¹ of data*, [arXiv:0911.3930](#) [[SPIRES](#)].
- [9] LEP WORKING GROUP FOR HIGGS BOSON SEARCHES collaboration, R. Barate et al., *Search for the standard model Higgs boson at LEP*, *Phys. Lett. B* **565** (2003) 61 [[hep-ex/0306033](#)] [[SPIRES](#)].
- [10] J. March-Russell and F. Riva, *Signals of inflation in a friendly string landscape*, *JHEP* **07** (2006) 033 [[astro-ph/0604254](#)] [[SPIRES](#)].
- [11] A. Djouadi, J. Kalinowski and M. Spira, *HDECAY: a program for Higgs boson decays in the standard model and its supersymmetric extension*, *Comput. Phys. Commun.* **108** (1998) 56 [[hep-ph/9704448](#)] [[SPIRES](#)].
- [12] J.M. Butterworth et al., *The tools and MonteCarlo working group summary report*, in *Les Houches report of the “Tools and Monte Carlo” working group*, A. Djouadi, J. Kalinowski, M.M. Muhlleitner and M. Spira eds., France (2009) [[arXiv:1003.1643](#)] [[SPIRES](#)].
- [13] H.M. Georgi, S.L. Glashow, M.E. Machacek and D.V. Nanopoulos, *Higgs bosons from two gluon annihilation in proton proton collisions*, *Phys. Rev. Lett.* **40** (1978) 692 [[SPIRES](#)].
- [14] M. Dittmar and H.K. Dreiner, *How to find a Higgs boson with a mass between 155–180 GeV at the LHC*, *Phys. Rev. D* **55** (1997) 167 [[hep-ph/9608317](#)] [[SPIRES](#)].
- [15] A. Djouadi, M. Spira and P.M. Zerwas, *Production of Higgs bosons in proton colliders: QCD corrections*, *Phys. Lett. B* **264** (1991) 440 [[SPIRES](#)].
- [16] S. Dawson, *Radiative corrections to Higgs boson production*, *Nucl. Phys. B* **359** (1991) 283 [[SPIRES](#)].
- [17] D. Graudenz, M. Spira and P.M. Zerwas, *QCD corrections to Higgs boson production at proton proton colliders*, *Phys. Rev. Lett.* **70** (1993) 1372 [[SPIRES](#)].
- [18] M. Spira, A. Djouadi, D. Graudenz and P.M. Zerwas, *SUSY Higgs production at proton colliders*, *Phys. Lett. B* **318** (1993) 347 [[SPIRES](#)].
- [19] M. Spira, A. Djouadi, D. Graudenz and P.M. Zerwas, *Higgs boson production at the LHC*, *Nucl. Phys. B* **453** (1995) 17 [[hep-ph/9504378](#)] [[SPIRES](#)].
- [20] M. Spira, *QCD effects in Higgs physics*, *Fortsch. Phys.* **46** (1998) 203 [[hep-ph/9705337](#)] [[SPIRES](#)].
- [21] R.V. Harlander and W.B. Kilgore, *Next-to-next-to-leading order Higgs production at hadron colliders*, *Phys. Rev. Lett.* **88** (2002) 201801 [[hep-ph/0201206](#)] [[SPIRES](#)].
- [22] C. Anastasiou and K. Melnikov, *Higgs boson production at hadron colliders in NNLO QCD*, *Nucl. Phys. B* **646** (2002) 220 [[hep-ph/0207004](#)] [[SPIRES](#)].
- [23] V. Ravindran, J. Smith and W.L. van Neerven, *NNLO corrections to the total cross section for Higgs boson production in hadron hadron collisions*, *Nucl. Phys. B* **665** (2003) 325 [[hep-ph/0302135](#)] [[SPIRES](#)].
- [24] S. Catani, D. de Florian, M. Grazzini and P. Nason, *Soft-gluon resummation for Higgs boson production at hadron colliders*, *JHEP* **07** (2003) 028 [[hep-ph/0306211](#)] [[SPIRES](#)].

- [25] D. de Florian and M. Grazzini, *Higgs production through gluon fusion: updated cross sections at the Tevatron and the LHC*, *Phys. Lett. B* **674** (2009) 291 [[arXiv:0901.2427](#)] [[SPIRES](#)].
- [26] C. Anastasiou, G. Dissertori, M. Grazzini, F. Stockli and B.R. Webber, *Perturbative QCD effects and the search for a $H \rightarrow WW \rightarrow \ell\nu\ell\nu$ signal at the Tevatron*, *JHEP* **08** (2009) 099 [[arXiv:0905.3529](#)] [[SPIRES](#)].
- [27] C. Anastasiou, R. Boughezal and F. Petriello, *Mixed QCD-electroweak corrections to Higgs boson production in gluon fusion*, *JHEP* **04** (2009) 003 [[arXiv:0811.3458](#)] [[SPIRES](#)].
- [28] A. Djouadi and P. Gambino, *Leading electroweak correction to Higgs boson production at proton colliders*, *Phys. Rev. Lett.* **73** (1994) 2528 [[hep-ph/9406432](#)] [[SPIRES](#)].
- [29] U. Aglietti, R. Bonciani, G. Degrossi and A. Vicini, *Two-loop light fermion contribution to Higgs production and decays*, *Phys. Lett. B* **595** (2004) 432 [[hep-ph/0404071](#)] [[SPIRES](#)].
- [30] G. Degrossi and F. Maltoni, *Two-loop electroweak corrections to Higgs production at hadron colliders*, *Phys. Lett. B* **600** (2004) 255 [[hep-ph/0407249](#)] [[SPIRES](#)].
- [31] S. Actis, G. Passarino, C. Sturm and S. Uccirati, *NLO electroweak corrections to Higgs boson production at hadron colliders*, *Phys. Lett. B* **670** (2008) 12 [[arXiv:0809.1301](#)] [[SPIRES](#)].
- [32] S. Actis, G. Passarino, C. Sturm and S. Uccirati, *NNLO computational techniques: the cases $H \rightarrow \gamma\gamma$ and $H \rightarrow gg$* , *Nucl. Phys. B* **811** (2009) 182 [[arXiv:0809.3667](#)] [[SPIRES](#)].
- [33] S.L. Glashow, D.V. Nanopoulos and A. Yildiz, *Associated production of Higgs bosons and Z particles*, *Phys. Rev. D* **18** (1978) 1724 [[SPIRES](#)].
- [34] A. Stange, W.J. Marciano and S. Willenbrock, *Associated production of Higgs and weak bosons, with $H \rightarrow b\bar{b}$, at hadron colliders*, *Phys. Rev. D* **50** (1994) 4491 [[hep-ph/9404247](#)] [[SPIRES](#)].
- [35] G. Altarelli, R.K. Ellis and G. Martinelli, *Large perturbative corrections to the Drell-Yan process in QCD*, *Nucl. Phys. B* **157** (1979) 461 [[SPIRES](#)].
- [36] J. Kubar-André and F.E. Paige, *Gluon corrections to the Drell-Yan model*, *Phys. Rev. D* **19** (1979) 221 [[SPIRES](#)].
- [37] T. Han and S. Willenbrock, *QCD correction to the $pp \rightarrow WH$ and ZH total cross-sections*, *Phys. Lett. B* **273** (1991) 167 [[SPIRES](#)].
- [38] J. Ohnemus and W.J. Stirling, *Order α_s corrections to the differential cross-section for the WH intermediate mass Higgs signal*, *Phys. Rev. D* **47** (1993) 2722 [[SPIRES](#)].
- [39] A. Djouadi and M. Spira, *SUSY-QCD corrections to Higgs boson production at hadron colliders*, *Phys. Rev. D* **62** (2000) 014004 [[hep-ph/9912476](#)] [[SPIRES](#)].
- [40] O. Brein, A. Djouadi and R. Harlander, *NNLO QCD corrections to the Higgs-strahlung processes at hadron colliders*, *Phys. Lett. B* **579** (2004) 149 [[hep-ph/0307206](#)] [[SPIRES](#)].
- [41] M.L. Ciccolini, S. Dittmaier and M. Krämer, *Electroweak radiative corrections to associated WH and ZH production at hadron colliders*, *Phys. Rev. D* **68** (2003) 073003 [[hep-ph/0306234](#)] [[SPIRES](#)].
- [42] A.D. Martin, W.J. Stirling, R.S. Thorne and G. Watt, *Parton distributions for the LHC*, *Eur. Phys. J. C* **63** (2009) 189 [[arXiv:0901.0002](#)] [[SPIRES](#)].

- [43] *Martin-Stirling-Thorne-Watt parton distribution functions homepage*, <http://projects.hepforge.org/mstwpdf/>.
- [44] R.S. Thorne, A.D. Martin, W.J. Stirling and G. Watt, *The effects of combined HERA and recent Tevatron $W \rightarrow \ell\nu$ charge asymmetry data on the MSTW PDFs*, [arXiv:1006.2753](https://arxiv.org/abs/1006.2753) [SPIRES].
- [45] O. Brein et al., *Precision calculations for associated WH and ZH production at hadron colliders*, [hep-ph/0402003](https://arxiv.org/abs/hep-ph/0402003) [SPIRES].
- [46] HIGGS WORKING GROUP collaboration, K.A. Assamagan et al., *The Higgs working group: summary report 2003*, [hep-ph/0406152](https://arxiv.org/abs/hep-ph/0406152) [SPIRES].
- [47] A.D. Martin, R.G. Roberts, W.J. Stirling and R.S. Thorne, *NNLO global parton analysis*, *Phys. Lett. B* **531** (2002) 216 [[hep-ph/0201127](https://arxiv.org/abs/hep-ph/0201127)] [SPIRES].
- [48] D.R.T. Jones and S.T. Petcov, *Heavy Higgs bosons at LEP*, *Phys. Lett. B* **84** (1979) 440 [SPIRES].
- [49] R.N. Cahn and S. Dawson, *Production of very massive Higgs bosons*, *Phys. Lett. B* **136** (1984) 196 [Erratum *ibid.* **B 138** (1984) 464] [SPIRES].
- [50] K. Hikasa, *Self-consistent boundary conditions*, *Phys. Lett. B* **164** (1985) 341.
- [51] G. Altarelli, B. Mele and F. Pitolli, *Heavy Higgs production at future colliders*, *Nucl. Phys. B* **287** (1987) 205 [SPIRES].
- [52] T. Han, G. Valencia and S. Willenbrock, *Structure function approach to vector boson scattering in pp collisions*, *Phys. Rev. Lett.* **69** (1992) 3274 [[hep-ph/9206246](https://arxiv.org/abs/hep-ph/9206246)] [SPIRES].
- [53] T. Figy, C. Oleari and D. Zeppenfeld, *Next-to-leading order jet distributions for Higgs boson production via weak-boson fusion*, *Phys. Rev. D* **68** (2003) 073005 [[hep-ph/0306109](https://arxiv.org/abs/hep-ph/0306109)] [SPIRES].
- [54] R. Raitio and W.W. Wada, *Higgs boson production at large transverse momentum in QCD*, *Phys. Rev. D* **19** (1979) 941 [SPIRES].
- [55] Z. Kunszt, *Associated production of heavy Higgs boson with top quarks*, *Nucl. Phys. B* **247** (1984) 339 [SPIRES].
- [56] J.N. Ng and P. Zakarauskas, *A QCD parton calculation of conjoined production of Higgs bosons and heavy flavors in $p\bar{p}$ collision*, *Phys. Rev. D* **29** (1984) 876 [SPIRES].
- [57] W. Beenakker et al., *Higgs radiation off top quarks at the Tevatron and the LHC*, *Phys. Rev. Lett.* **87** (2001) 201805 [[hep-ph/0107081](https://arxiv.org/abs/hep-ph/0107081)] [SPIRES].
- [58] W. Beenakker et al., *NLO QCD corrections to $t\bar{t}H$ production in hadron collisions*, *Nucl. Phys. B* **653** (2003) 151 [[hep-ph/0211352](https://arxiv.org/abs/hep-ph/0211352)] [SPIRES].
- [59] L. Reina and S. Dawson, *Next-to-leading order results for $t\bar{t}H$ production at the Tevatron*, *Phys. Rev. Lett.* **87** (2001) 201804 [[hep-ph/0107101](https://arxiv.org/abs/hep-ph/0107101)] [SPIRES].
- [60] S. Dawson, L.H. Orr, L. Reina and D. Wackerroth, *Associated top quark Higgs boson production at the LHC*, *Phys. Rev. D* **67** (2003) 071503 [[hep-ph/0211438](https://arxiv.org/abs/hep-ph/0211438)] [SPIRES].
- [61] P.M. Nadolsky et al., *Implications of CTEQ global analysis for collider observables*, *Phys. Rev. D* **78** (2008) 013004 [[arXiv:0802.0007](https://arxiv.org/abs/0802.0007)] [SPIRES].
- [62] *CTEQ: the Coordinated Theoretical-Experimental project on QCD homepage*, <http://www.phys.psu.edu/~cteq/>.

- [63] S. Alekhin, J. Blumlein, S. Klein and S. Moch, *The 3-, 4- and 5-flavor NNLO parton from deep-inelastic-scattering data and at hadron colliders*, *Phys. Rev. D* **81** (2010) 014032 [[arXiv:0908.2766](#)] [[SPIRES](#)].
- [64] *The Nucleon Parton Distribution Functions homepage*, <https://mail.ihep.ru/~alekhin/pdfs.html>.
- [65] M. Spira, *HIGLU: a program for the calculation of the total Higgs production cross section at hadron colliders via gluon fusion including QCD corrections*, [hep-ph/9510347](#) [[SPIRES](#)].
- [66] *Programs for SM and MSSM Higgs boson production at hadron colliders*, <http://people.web.psi.ch/spira/proglist.html>.
- [67] M. Krämer, E. Laenen and M. Spira, *Soft gluon radiation in Higgs boson production at the LHC*, *Nucl. Phys. B* **511** (1998) 523 [[hep-ph/9611272](#)] [[SPIRES](#)].
- [68] S. Moch and A. Vogt, *Higher-order soft corrections to lepton pair and Higgs boson production*, *Phys. Lett. B* **631** (2005) 48 [[hep-ph/0508265](#)] [[SPIRES](#)].
- [69] V. Ravindran, *Higher-order threshold effects to inclusive processes in QCD*, *Nucl. Phys. B* **752** (2006) 173 [[hep-ph/0603041](#)] [[SPIRES](#)].
- [70] A. Idilbi, X.-D. Ji, J.-P. Ma and F. Yuan, *Threshold resummation for Higgs production in effective field theory*, *Phys. Rev. D* **73** (2006) 077501 [[hep-ph/0509294](#)] [[SPIRES](#)].
- [71] E. Laenen and L. Magnea, *Threshold resummation for electroweak annihilation from DIS data*, *Phys. Lett. B* **632** (2006) 270 [[hep-ph/0508284](#)] [[SPIRES](#)].
- [72] V. Ahrens, T. Becher, M. Neubert and L.L. Yang, *Renormalization-group improved prediction for Higgs production at hadron colliders*, *Eur. Phys. J. C* **62** (2009) 333 [[arXiv:0809.4283](#)] [[SPIRES](#)].
- [73] G. Corcella and L. Magnea, *Soft-gluon resummation effects on parton distributions*, *Phys. Rev. D* **72** (2005) 074017 [[hep-ph/0506278](#)] [[SPIRES](#)].
- [74] V. Ravindran, J. Smith and W.L. van Neerven, *Differential cross sections for Higgs production*, *Mod. Phys. Lett. A* **18** (2003) 1721 [[hep-ph/0307005](#)] [[SPIRES](#)].
- [75] C. Anastasiou, K. Melnikov and F. Petriello, *Fully differential Higgs boson production and the di-photon signal through next-to-next-to-leading order*, *Nucl. Phys. B* **724** (2005) 197 [[hep-ph/0501130](#)] [[SPIRES](#)].
- [76] S. Catani and M. Grazzini, *An NNLO subtraction formalism in hadron collisions and its application to Higgs boson production at the LHC*, *Phys. Rev. Lett.* **98** (2007) 222002 [[hep-ph/0703012](#)] [[SPIRES](#)].
- [77] C. Anastasiou, S. Bucherer and Z. Kunszt, *HPro: a NLO MonteCarlo for Higgs production via gluon fusion with finite heavy quark masses*, *JHEP* **10** (2009) 068 [[arXiv:0907.2362](#)] [[SPIRES](#)].
- [78] S.D. Drell and T.-M. Yan, *Massive lepton pair production in hadron-hadron collisions at high-energies*, *Phys. Rev. Lett.* **25** (1970) 316 [[SPIRES](#)].
- [79] R. Hamberg, W.L. van Neerven and T. Matsuura, *A complete calculation of the order α_s^2 correction to the Drell-Yan K factor*, *Nucl. Phys. B* **359** (1991) 343 [*Erratum ibid.* **B 644** (2002) 403] [[SPIRES](#)].
- [80] M. Ciccolini, A. Denner and S. Dittmaier, *Electroweak and QCD corrections to Higgs production via vector-boson fusion at the LHC*, *Phys. Rev. D* **77** (2008) 013002 [[arXiv:0710.4749](#)] [[SPIRES](#)].

- [81] TEVATRON ELECTROWEAK WORKING GROUP AND CDF AND D0 collaboration, *Combination of CDF and D0 results on the mass of the top quark*, [arXiv:0903.2503](#) [SPIRES].
- [82] M. Grazzini, *Higgs cross section: compute reference SM Higgs production cross sections webpage*, <http://theory.fi.infn.it/cgi-bin/hresum.pl>.
- [83] U. Aglietti et al., *Tevatron for LHC report: Higgs*, [hep-ph/0612172](#) [SPIRES].
- [84] TEV4LHC HIGGS WORKING GROUP collaboration, *Standard model Higgs cross sections at hadron colliders webpage*, <http://maltoni.web.cern.ch/maltoni/TeV4LHC/SM.html>.
- [85] A. Bredenstein, A. Denner, S. Dittmaier and M.M. Weber, *Precise predictions for the Higgs-boson decay $H \rightarrow WW/ZZ \rightarrow 4$ leptons*, *Phys. Rev. D* **74** (2006) 013004 [[hep-ph/0604011](#)] [SPIRES].
- [86] A. Bredenstein, A. Denner, S. Dittmaier and M.M. Weber, *Radiative corrections to the semileptonic and hadronic Higgs-boson decays $H \rightarrow WW/ZZ \rightarrow 4$ fermions*, *JHEP* **02** (2007) 080 [[hep-ph/0611234](#)] [SPIRES].
- [87] K. Melnikov and F. Petriello, *The W boson production cross section at the LHC through $O(\alpha_s^2)$* , *Phys. Rev. Lett.* **96** (2006) 231803 [[hep-ph/0603182](#)] [SPIRES].
- [88] S. Catani, L. Cieri, G. Ferrera, D. de Florian and M. Grazzini, *Vector boson production at hadron colliders: a fully exclusive QCD calculation at NNLO*, *Phys. Rev. Lett.* **103** (2009) 082001 [[arXiv:0903.2120](#)] [SPIRES].
- [89] J. Ohnemus, *An order α_s calculation of hadronic W^-W^+ production*, *Phys. Rev. D* **44** (1991) 1403 [SPIRES].
- [90] S. Frixione, P. Nason and G. Ridolfi, *Strong corrections to WZ production at hadron colliders*, *Nucl. Phys. B* **383** (1992) 3 [SPIRES].
- [91] S. Frixione, *A next-to-leading order calculation of the cross-section for the production of W^+W^- pairs in hadronic collisions*, *Nucl. Phys. B* **410** (1993) 280 [SPIRES].
- [92] U. Baur, T. Han and J. Ohnemus, *QCD corrections to hadronic $W\gamma$ production with nonstandard $WW\gamma$ couplings*, *Phys. Rev. D* **48** (1993) 5140 [[hep-ph/9305314](#)] [SPIRES].
- [93] L.J. Dixon, Z. Kunszt and A. Signer, *Vector boson pair production in hadronic collisions at order α_s : lepton correlations and anomalous couplings*, *Phys. Rev. D* **60** (1999) 114037 [[hep-ph/9907305](#)] [SPIRES].
- [94] M. Cacciari, S. Frixione, M.L. Mangano, P. Nason and G. Ridolfi, *Updated predictions for the total production cross sections of top and of heavier quark pairs at the Tevatron and at the LHC*, *JHEP* **09** (2008) 127 [[arXiv:0804.2800](#)] [SPIRES].
- [95] N. Kidonakis and R. Vogt, *The theoretical top quark cross section at the Tevatron and the LHC*, *Phys. Rev. D* **78** (2008) 074005 [[arXiv:0805.3844](#)] [SPIRES].
- [96] S. Moch and P. Uwer, *Theoretical status and prospects for top-quark pair production at hadron colliders*, *Phys. Rev. D* **78** (2008) 034003 [[arXiv:0804.1476](#)] [SPIRES].
- [97] S. Dittmaier, M. Krämer and M. Spira, *Higgs radiation off bottom quarks at the Tevatron and the LHC*, *Phys. Rev. D* **70** (2004) 074010 [[hep-ph/0309204](#)] [SPIRES].
- [98] J.M. Campbell, R.K. Ellis, F. Maltoni and S. Willenbrock, *Higgs boson production in association with a single bottom quark*, *Phys. Rev. D* **67** (2003) 095002 [[hep-ph/0204093](#)] [SPIRES].

- [99] R.V. Harlander and W.B. Kilgore, *Higgs boson production in bottom quark fusion at next-to-next-to-leading order*, *Phys. Rev. D* **68** (2003) 013001 [[hep-ph/0304035](#)] [[SPIRES](#)].
- [100] F. Maltoni, Z. Sullivan and S. Willenbrock, *Higgs-boson production via bottom-quark fusion*, *Phys. Rev. D* **67** (2003) 093005 [[hep-ph/0301033](#)] [[SPIRES](#)].
- [101] J. Campbell et al., *Higgs boson production in association with bottom quarks*, in *The Higgs working group: summary report 2003*, HIGGS WORKING GROUP collaboration, K.A. Assamagan et al., France (2003), pg. 5 [[hep-ph/0406152](#)] [[SPIRES](#)].
- [102] V. Ravindran, J. Smith and W.L. van Neerven, *NNLO corrections to the Higgs production cross section*, *Nucl. Phys. (Proc. Suppl.)* **135** (2004) 35 [[hep-ph/0405263](#)] [[SPIRES](#)].
- [103] R.V. Harlander and W.B. Kilgore, *Production of a pseudo-scalar Higgs boson at hadron colliders at next-to-next-to leading order*, *JHEP* **10** (2002) 017 [[hep-ph/0208096](#)] [[SPIRES](#)].
- [104] A. Cafarella, C. Corianò, M. Guzzi and J. Smith, *On the scale variation of the total cross section for Higgs production at the LHC and at the Tevatron*, *Eur. Phys. J. C* **47** (2006) 703 [[hep-ph/0510179](#)] [[SPIRES](#)].
- [105] A. Djouadi, *The Anatomy of electro-weak symmetry breaking. II. The Higgs bosons in the minimal supersymmetric model*, *Phys. Rept.* **459** (2008) 1 [[hep-ph/0503173](#)] [[SPIRES](#)].
- [106] R.V. Harlander and K.J. Ozeren, *Finite top mass effects for hadronic Higgs production at next-to-next-to-leading order*, *JHEP* **11** (2009) 088 [[arXiv:0909.3420](#)] [[SPIRES](#)].
- [107] A. Pak, M. Rogal and M. Steinhauser, *Finite top quark mass effects in NNLO Higgs boson production at LHC*, *JHEP* **02** (2010) 025 [[arXiv:0911.4662](#)] [[SPIRES](#)].
- [108] R.V. Harlander, H. Mantler, S. Marzani and K.J. Ozeren, *Higgs production in gluon fusion at next-to-next-to-leading order QCD for finite top mass*, *Eur. Phys. J. C* **66** (2010) 359 [[arXiv:0912.2104](#)] [[SPIRES](#)].
- [109] S. Marzani, R.D. Ball, V. Del Duca, S. Forte and A. Vicini, *Higgs production via gluon-gluon fusion with finite top mass beyond next-to-leading order*, *Nucl. Phys. B* **800** (2008) 127 [[arXiv:0801.2544](#)] [[SPIRES](#)].
- [110] A.D. Martin, W.J. Stirling, R.S. Thorne and G. Watt, *Uncertainties on α_S in global PDF analyses and implications for predicted hadronic cross sections*, *Eur. Phys. J. C* **64** (2009) 653 [[arXiv:0905.3531](#)] [[SPIRES](#)].
- [111] A. Djouadi and S. Ferrag, *PDF uncertainties in Higgs production at hadron colliders*, *Phys. Lett. B* **586** (2004) 345 [[hep-ph/0310209](#)] [[SPIRES](#)].
- [112] NNPDF collaboration, R.D. Ball et al., *Precision determination of electroweak parameters and the strange content of the proton from neutrino deep-inelastic scattering*, *Nucl. Phys. B* **823** (2009) 195 [[arXiv:0906.1958](#)] [[SPIRES](#)].
- [113] P. Jimenez-Delgado and E. Reya, *Variable flavor number parton distributions and weak gauge and Higgs boson production at hadron colliders at NNLO of QCD*, *Phys. Rev. D* **80** (2009) 114011 [[arXiv:0909.1711](#)] [[SPIRES](#)].
- [114] M. Grazzini, *QCD effects in Higgs boson production at hadron colliders*, *PoS(RADCOR2009)047* [[arXiv:1001.3766](#)] [[SPIRES](#)].
- [115] M. Buza, Y. Matiounine, J. Smith and W.L. van Neerven, *Charm electroproduction viewed in the variable-flavour number scheme versus fixed-order perturbation theory*, *Eur. Phys. J. C* **1** (1998) 301 [[hep-ph/9612398](#)] [[SPIRES](#)].

- [116] S. Alekhin, *Parton distributions from deep-inelastic scattering data*, *Phys. Rev. D* **68** (2003) 014002 [[hep-ph/0211096](#)] [[SPIRES](#)].
- [117] CDF collaboration, T. Aaltonen et al., *Inclusive search for standard model Higgs boson production in the WW decay channel using the CDF II detector*, *Phys. Rev. Lett.* **104** (2010) 061803 [[arXiv:1001.4468](#)] [[SPIRES](#)].
- [118] D0 collaboration, V.M. Abazov et al., *Search for Higgs boson production in dilepton and missing energy final states with 5.4 fb^{-1} of $p\bar{p}$ collisions at $\sqrt{s} = 1.96 \text{ TeV}$* , *Phys. Rev. Lett.* **104** (2010) 061804 [[arXiv:1001.4481](#)] [[SPIRES](#)].
- [119] G. Bernardi et al., *Combined CDF and D0 upper limits on standard model Higgs boson production at high mass (155–200 GeV/c^2) with 3 fb^{-1} of data*, [arXiv:0808.0534](#) [[SPIRES](#)].
- [120] M. Dittmar, F. Pauss and D. Zurcher, *Towards a precise parton luminosity determination at the CERN LHC*, *Phys. Rev. D* **56** (1997) 7284 [[hep-ex/9705004](#)] [[SPIRES](#)].
- [121] D. Zeppenfeld, R. Kinnunen, A. Nikitenko and E. Richter-Was, *Measuring Higgs boson couplings at the LHC*, *Phys. Rev. D* **62** (2000) 013009 [[hep-ph/0002036](#)] [[SPIRES](#)].
- [122] M. Dührssen et al., *Extracting Higgs boson couplings from LHC data*, *Phys. Rev. D* **70** (2004) 113009 [[hep-ph/0406323](#)] [[SPIRES](#)].
- [123] C. Anastasiou, K. Melnikov and F. Petriello, *The gluon-fusion uncertainty in Higgs coupling extractions*, *Phys. Rev. D* **72** (2005) 097302 [[hep-ph/0509014](#)] [[SPIRES](#)].
- [124] J. Baglio et al., in preparation.
- [125] *Tevatron new phenomena & Higgs working group: responses to concerns about the theoretical modeling of the $gg \rightarrow H$ signal*, http://tevnpnwg.fnal.gov/results/SMHPubWinter2010/gghtheoryreplies_may2010.html.
- [126] CDF AND D0 collaboration, *Combined CDF and D0 upper limits on standard model Higgs-boson production with up to 6.7 fb^{-1} of data*, [arXiv:1007.4587](#) [[SPIRES](#)].
- [127] CDF AND D0 collaboration, B. Kiminster, *Higgs boson searches at the Tevatron*, talk given at *ICHEP 2010*, July 26 2010.
- [128] C. Anastasiou, *Higgs production via gluon fusion*, talk given at *Higgs Hunting workshop*, held in Orsay France July 29–31 2010, <http://indico.lal.in2p3.fr/conferenceDisplay.py?confid=1109>.
- [129] R. Thorne, *PDFs, constraints and searches at LHC*, talk given at *Higgs Hunting workshop*, held in Orsay France July 29–31 2010, <http://indico.lal.in2p3.fr/conferenceDisplay.py?confid=1109>.
- [130] The NNLO PDF sets can be found at *Official page of the H1 and ZEUS public combined results*, http://www.desy.de/h1zeus/combined_results.